Combining diving and reflected waves for velocity and impedance models building by waveform inversion

Romain Brossier[1], Wei Zhou[1], Stéphane Operto[2] and Jean Virieux[1]
romain.brossier@ujf-grenoble.fr

[1] Univ. Grenoble Alpes - CNRS, ISTerre, Grenoble, France
[2] Univ. Nice Sophia-Antipolis - CNRS, Géoazur, Sophia-Antipolis, France

Inverse problem meeting, Persyval Labex
Grenoble, 12 December 2014

Outline

Outline

- Quantitative tomography : reconstruction of Earth subsurface properties from remote measurements of seismic waves

$$\frac{\partial U}{\partial t} + \Lambda \frac{\partial U}{\partial x_i} = F_0$$

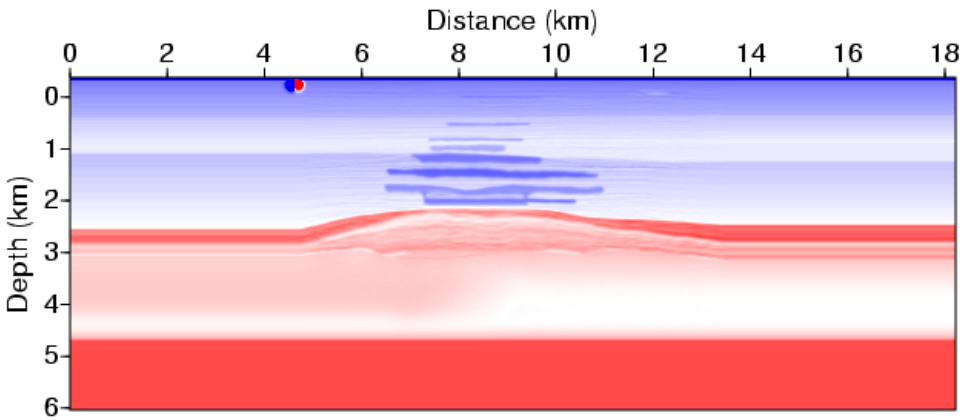

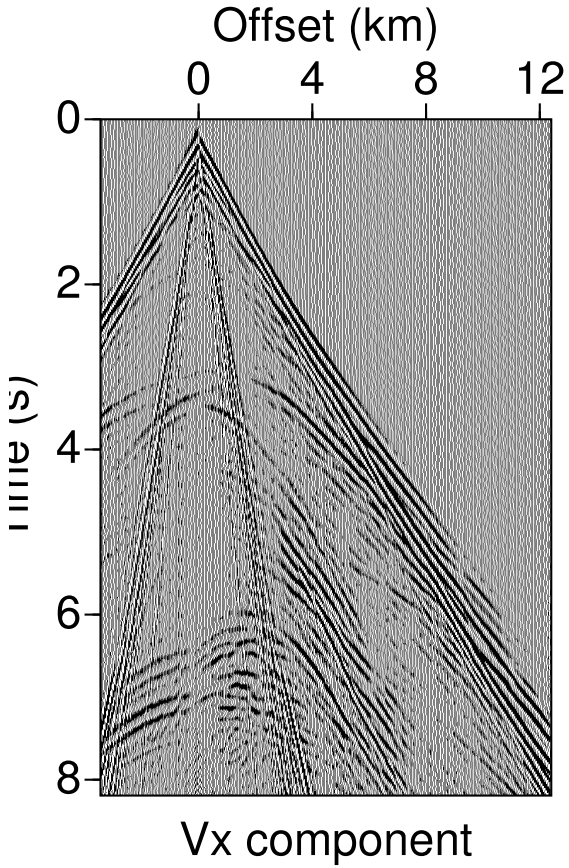

Seismic methods : which data ?

Different observables from data

- First arrival time tomography
- Reflection tomography
- Migration of reflected/scattered waves
- Refraction tomography
- Surface wave dispersion
- Amplitude analysis (AVO)
- ...

→ All limited information

Full Waveform Inversion (FWI)

- traveltime and amplitude of all arrivals

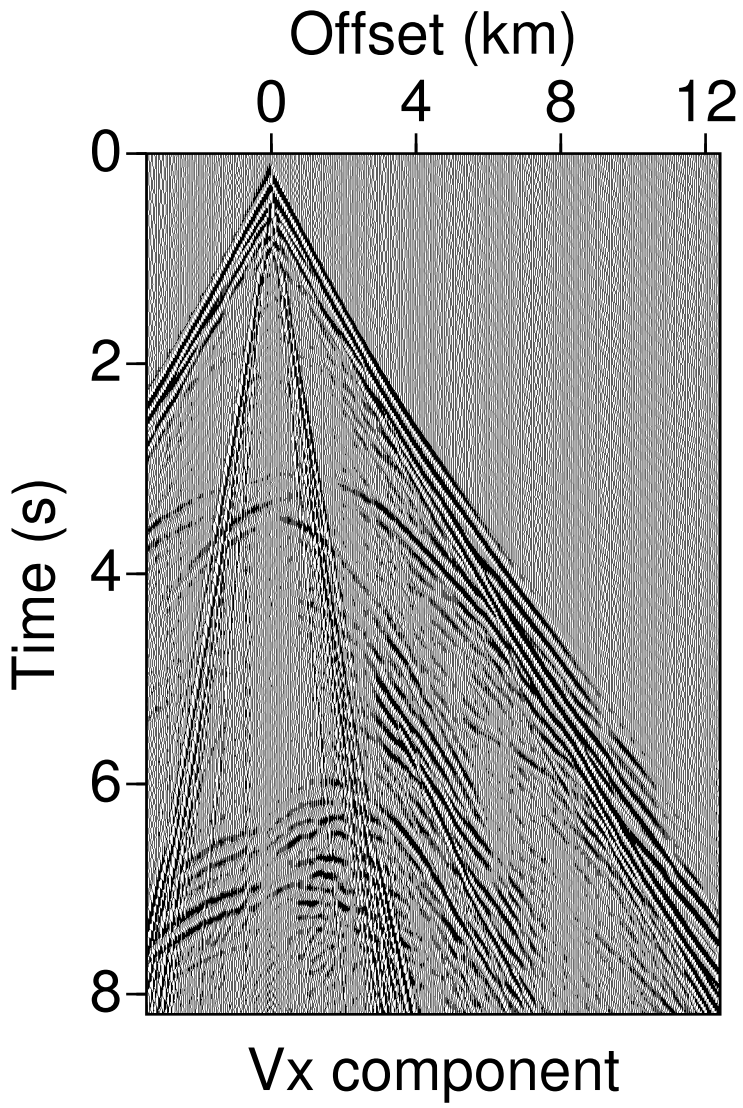

Full waveform inversion : principle

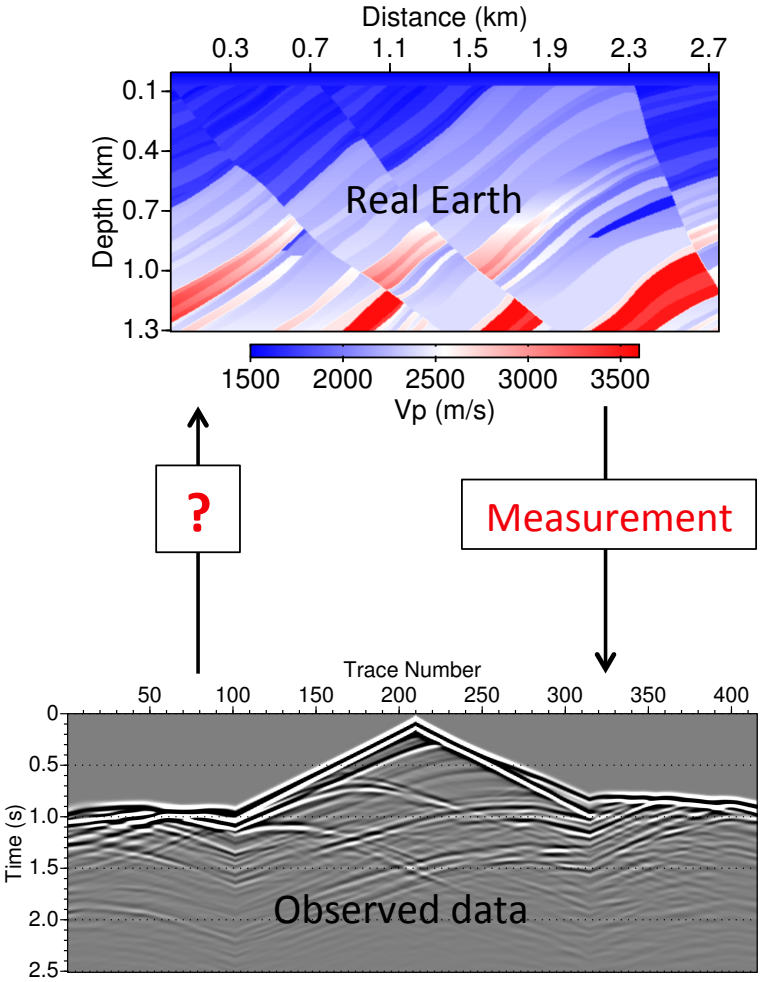

Full waveform inversion : principle

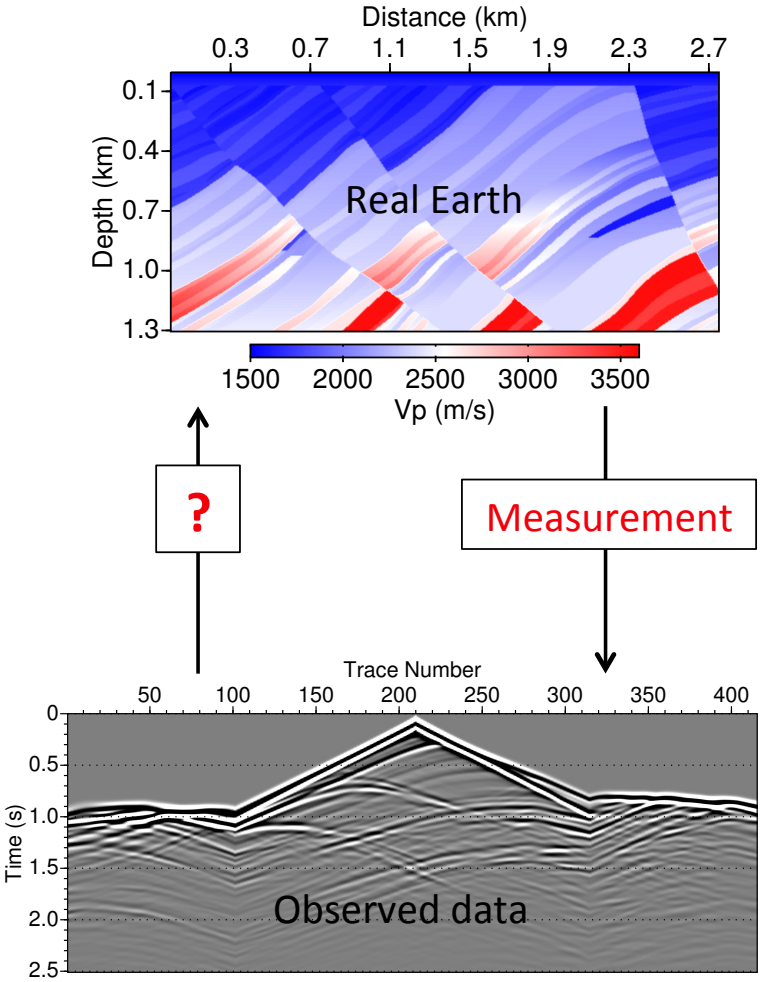

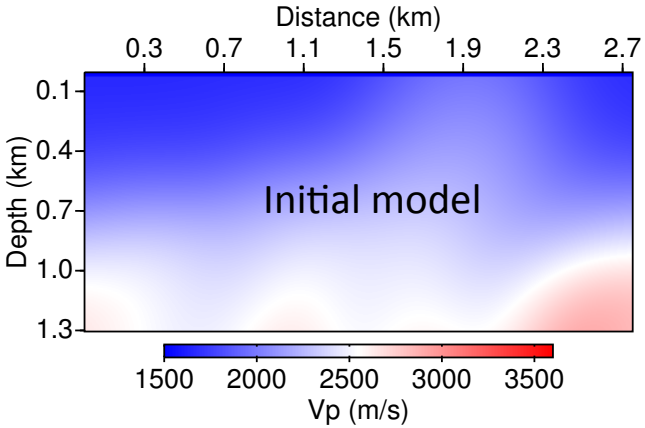

Full waveform inversion : principle

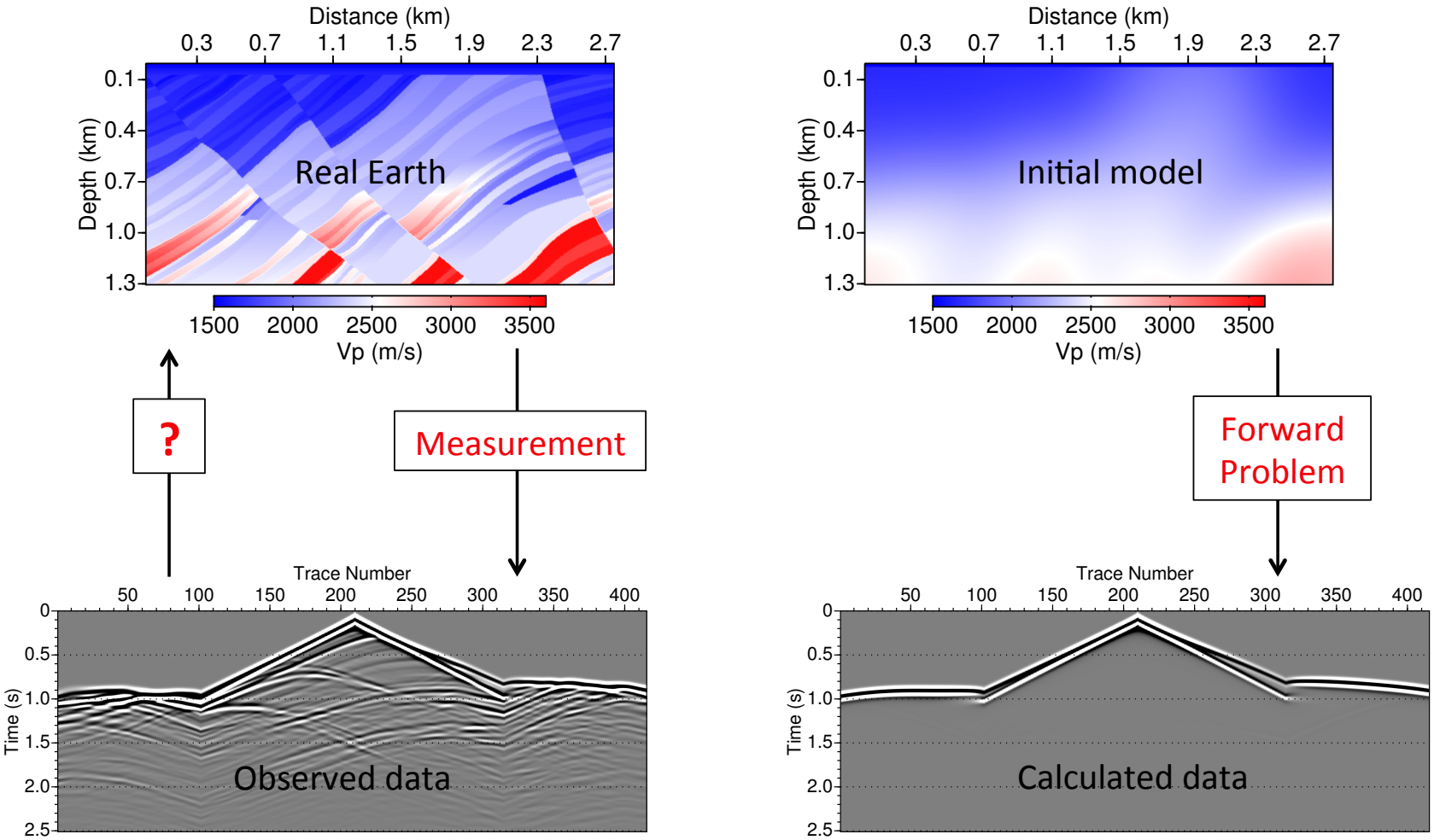

Full waveform inversion : principle

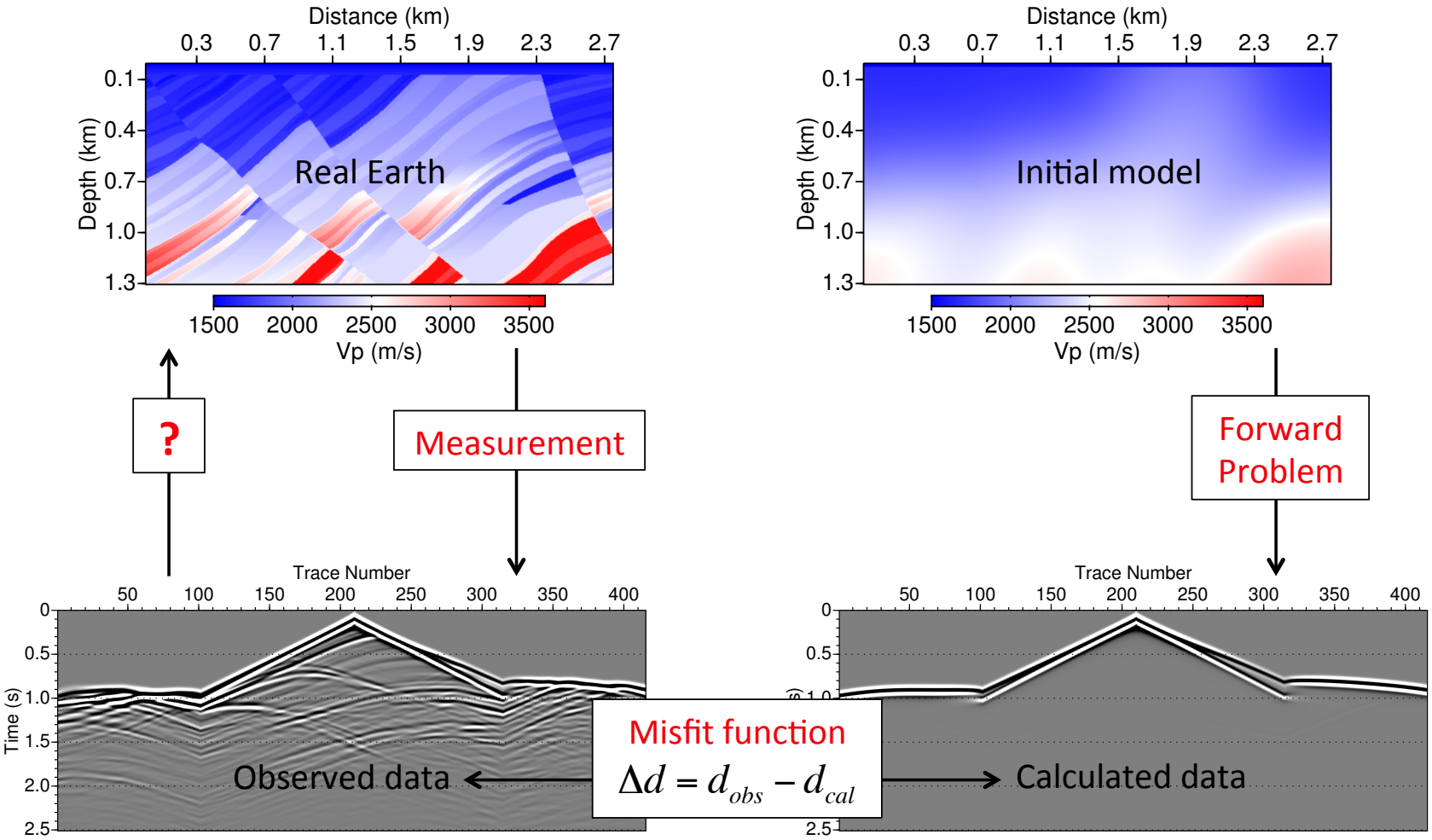

Full waveform inversion : principle

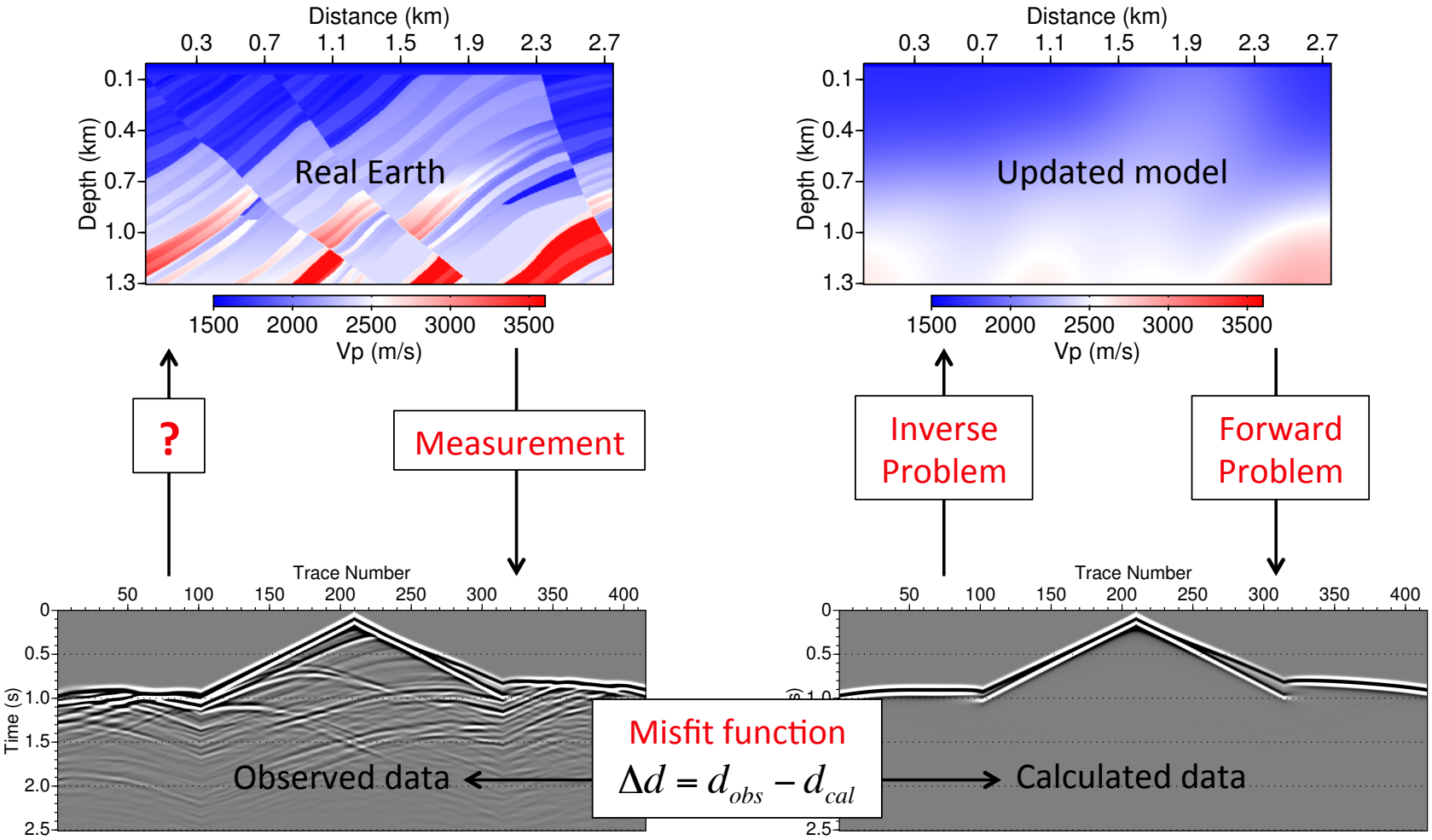

Full waveform inversion : principle

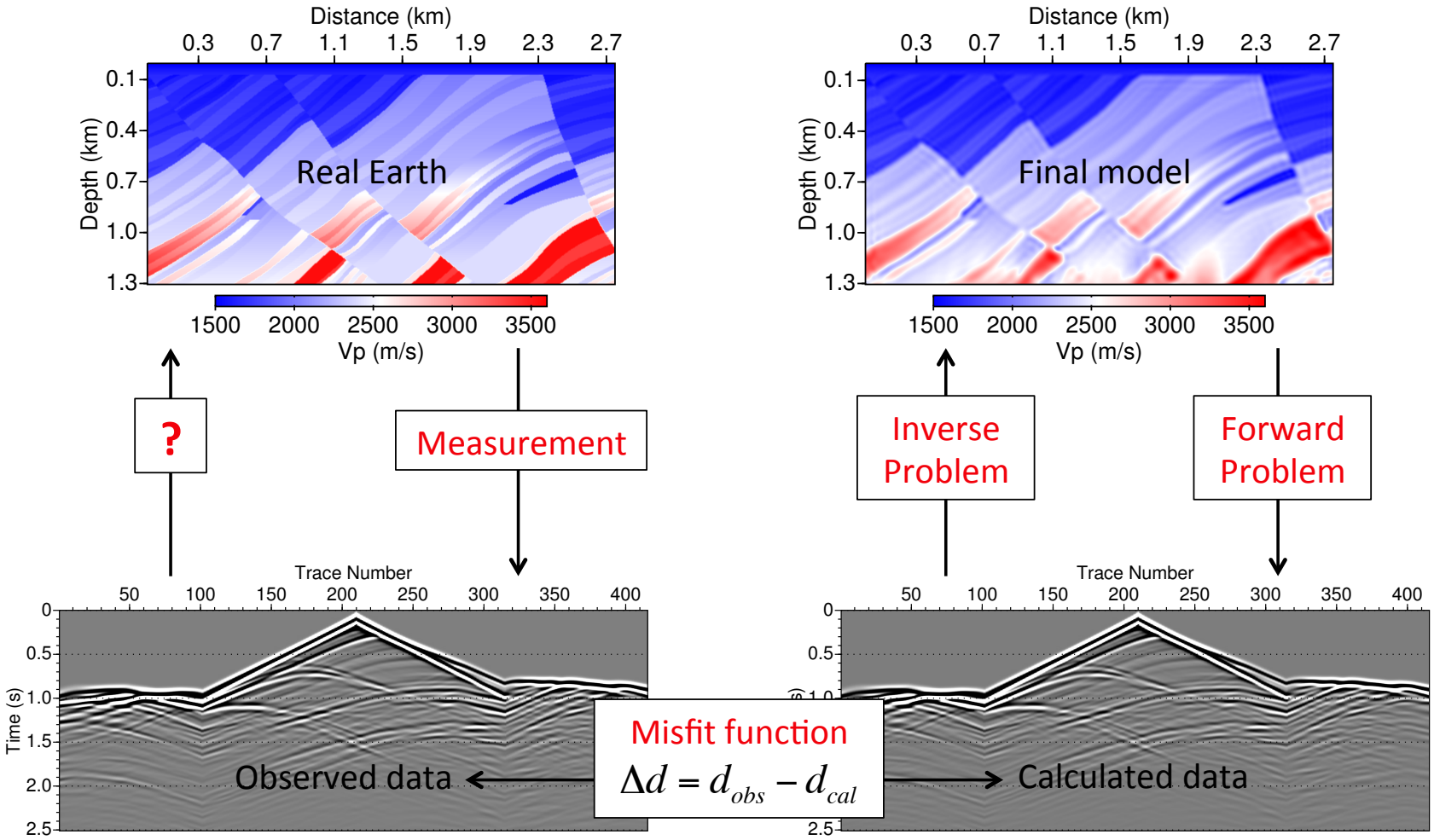

Full waveform inversion : workflow

Initial velocity model

m_0

Forward modeling

Wave equation

- *Finite differences*
- *Finite elements*

Synthetic data

d_{cal}

Observed data

d_{obs}

Calculate misfit

$$\Delta d(m) = d_{obs} - d_{cal}(m)$$

$$C(m) = \frac{1}{2}\|\Delta d(m)\|^2$$

(minimize L2 norm of difference)

Calculate Gradient and Hessian

$$C'(m) = g$$

$$C''(m) = H \text{ (approx.)}$$

Solved with adjoint method

Calculate model update

$$H\Delta m = -g$$

Inverse problem solved implicitly

Updated velocity model

$$m = m_0 + \Delta m$$

Iterative approach

Outline

FWI formulation

- FWI : data-fitting procedure which aims to use all the waveforms (Lailly, 1983; Tarantola, 1984; Pratt and Worthington, 1990; Virieux and Operto, 2009)
- Classical FWI misfit function

$$C_{classical} = \sum_{src,rec} \frac{1}{2} \| d_{obs}(t) - d_{pred}(t,m) \|^2 \tag{1}$$

- Lagrangian formulation with adjoint state technique to derive the gradient direction

$$\begin{aligned} L &= \sum_{src,rec} \frac{1}{2} \| d_{obs}(t) - d_{pred}(t) \|^2 + < \lambda_1(t) | d_{pred}(t) - Ru(t,\mathbf{x}) >_{src,rec,T} \\ &+ < \lambda_2(t,\mathbf{x}) | A(m)u(t,\mathbf{x}) - s(t,\mathbf{x}) >_{src,T} \end{aligned} \tag{2}$$

giving

$$\begin{aligned} A(m)u(t,\mathbf{x}) &= s(t,\mathbf{x}) \quad \rightarrow \text{state equation with initial condition} \\ A(m)^{\dagger}\lambda(t,\mathbf{x}) &= \sum_{rec} (d_{obs}(t) - d_{pred}(t)) \quad \rightarrow \text{adjoint equation with final condition} \end{aligned}$$

leading to the gradient expression (used to predict the descent direction)

$$G_{classical_i} = \sum_{src,rec} u(t,\mathbf{x}) \frac{\partial A(m)^{\dagger}}{\partial m_i} \lambda(t,\mathbf{x}) \tag{3}$$

where

FWI formulation

$$C_{classical} = \sum_{src,rec} \frac{1}{2} \| d_{obs}(t) - d_{pred}(t,m) \|^2 \qquad G_{classical_i} = \sum_{src,rec} u(t,\mathbf{x}) \frac{\partial A(m)^\dagger}{\partial m_i} \lambda(t,\mathbf{x})$$

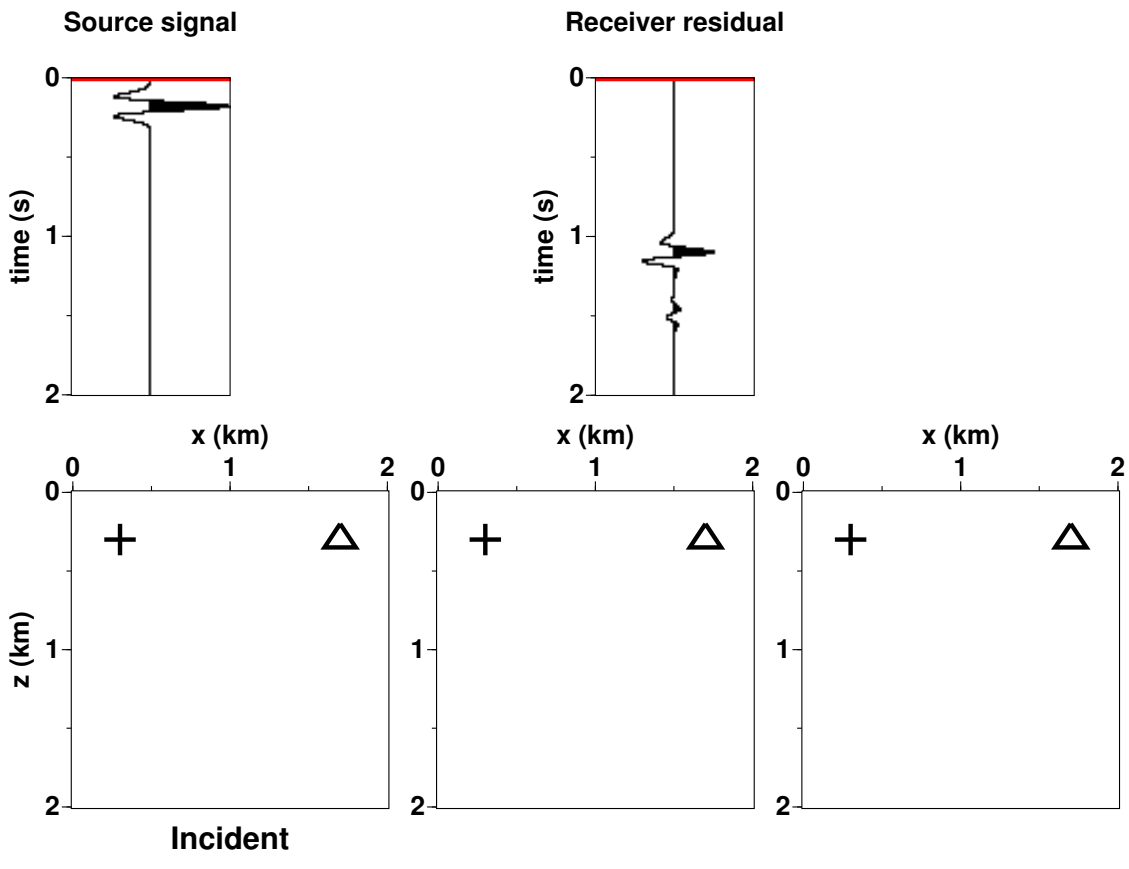

FWI formulation

$$C_{classical} = \sum_{src,rec} \frac{1}{2} \| d_{obs}(t) - d_{pred}(t,m) \|^2 \qquad G_{classical_i} = \sum_{src,rec} u(t,\mathbf{x}) \frac{\partial A(m)^\dagger}{\partial m_i} \lambda(t,\mathbf{x})$$

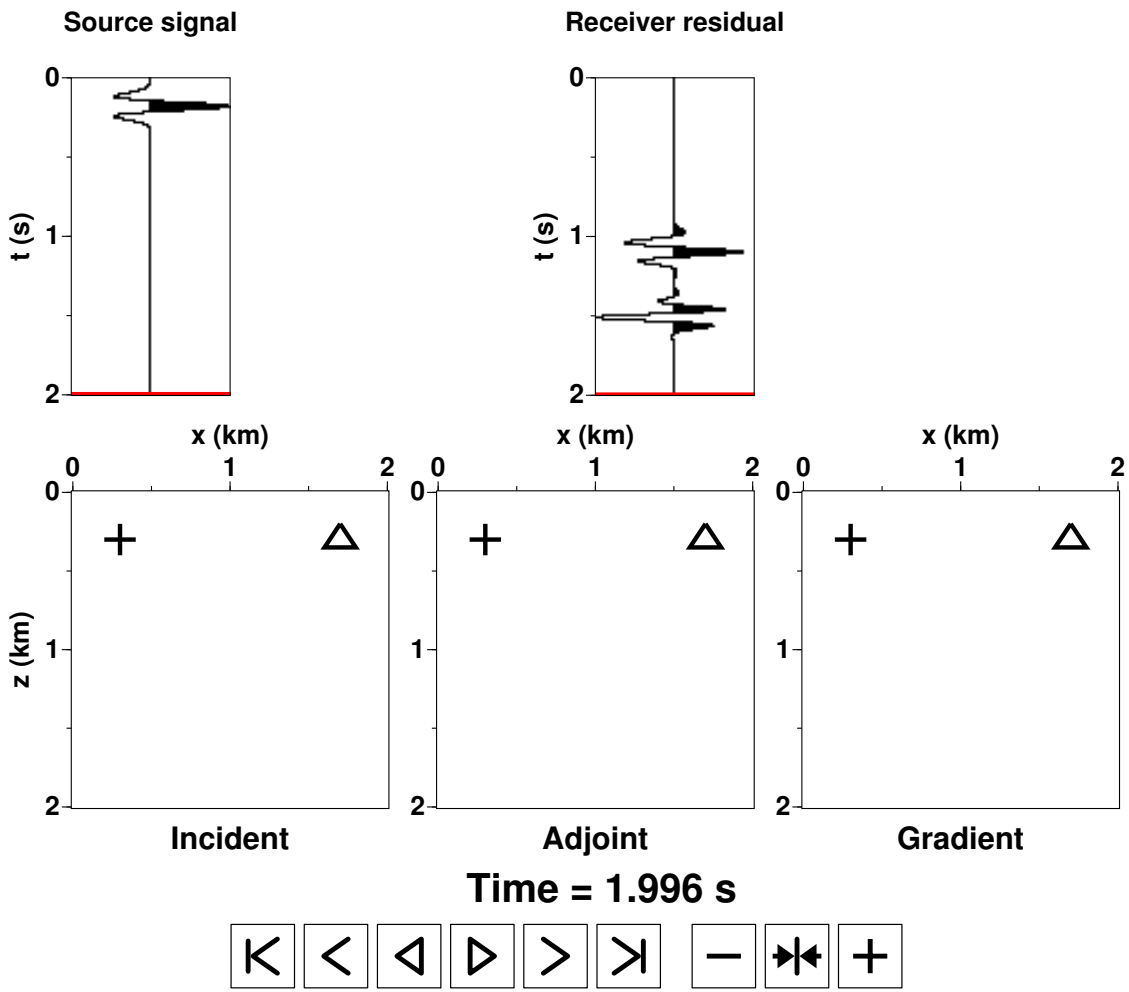

FWI intrinsic resolution

- in short, the model update can be seen as the zero-lag cross-correlation

$$G_{classical} = u \star \lambda \tag{4}$$

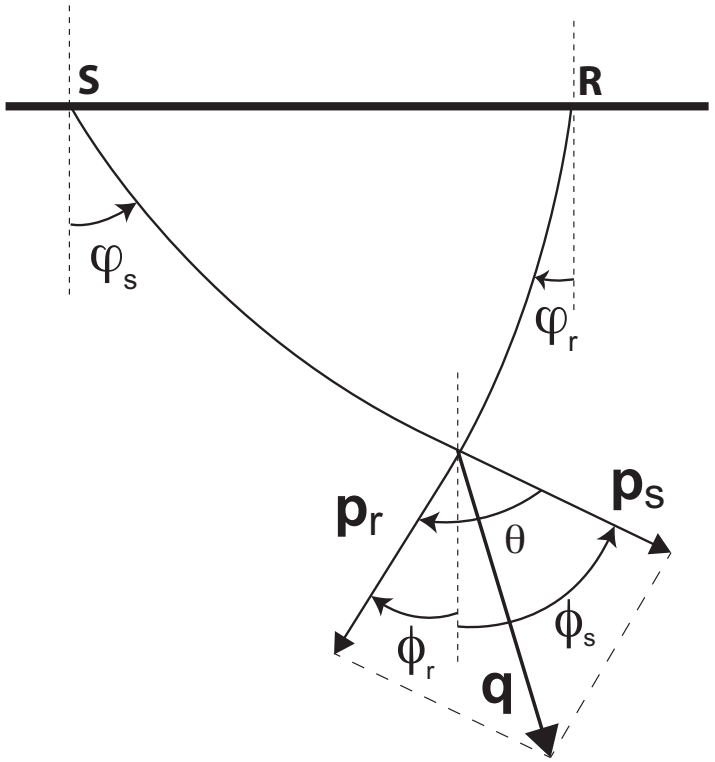

- FWI relies on the diffraction tomography principle (Devaney, 1982; Wu and Toksöz, 1987), the updated wavenumber is

$$\vec{\mathbf{k}} = \frac{2\omega}{c_0} \cos\left(\frac{\theta}{2}\right) \frac{\vec{\mathbf{q}}}{|\vec{\mathbf{q}}|}, \tag{5}$$

FWI resolution in practice (and associated issues)

$$\vec{\mathbf{k}} = \frac{2\omega}{c_0} \cos\left(\frac{\theta}{2}\right) \frac{\vec{\mathbf{q}}}{|\vec{\mathbf{q}}|},$$

- Shallow targets: A broadband of wavenumbers can be imaged thanks to the broad coverage of scattering angles θ provided by transmitted and reflected waves.
- Deep targets: illuminated by short-spread reflections only, leading to high-wavenumber imaging only.
  $\rightarrow$ lack of low-wavenumbers if very-low frequencies not available (often the case in practice)

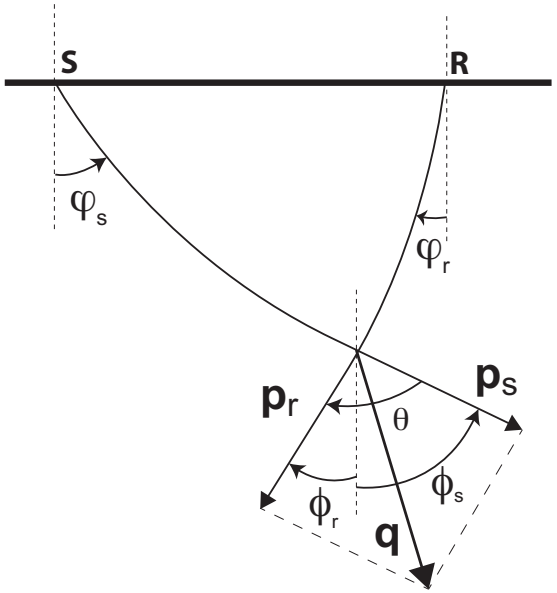

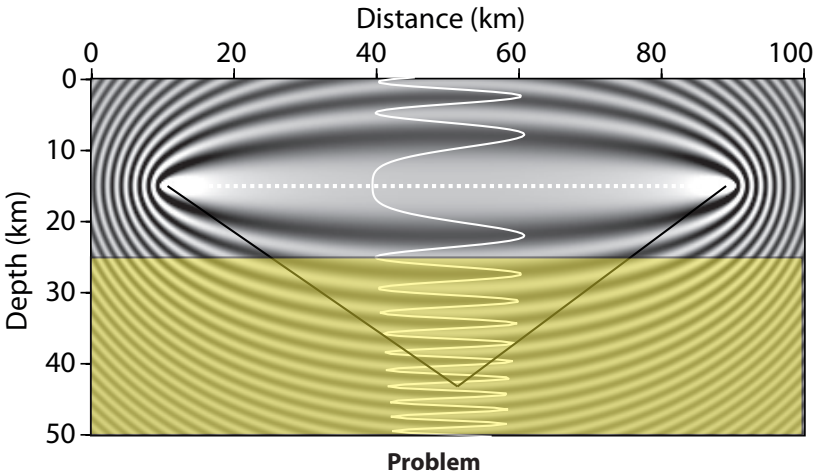

Problem
how to update the long wavelengths of the subsurface in the shaded area?

FWI resolution in practice (and associated issues)

Example of FWI gradient on realistic synthetic case

- Not enough low-frequencies
- limited offset-range : 6 km

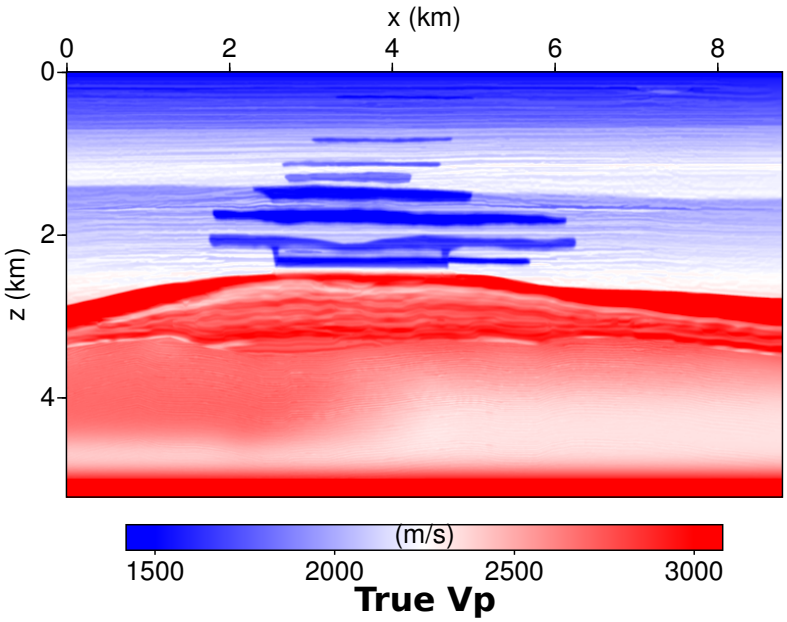

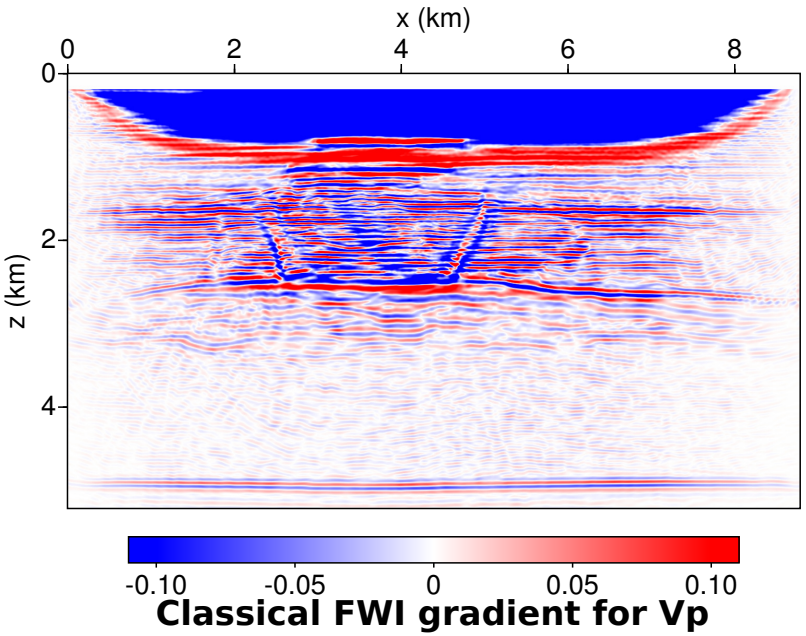

Outline

2D Imaging of the Nankai trough

- One of the early successfull application on real data, by Operto et al. (2006)

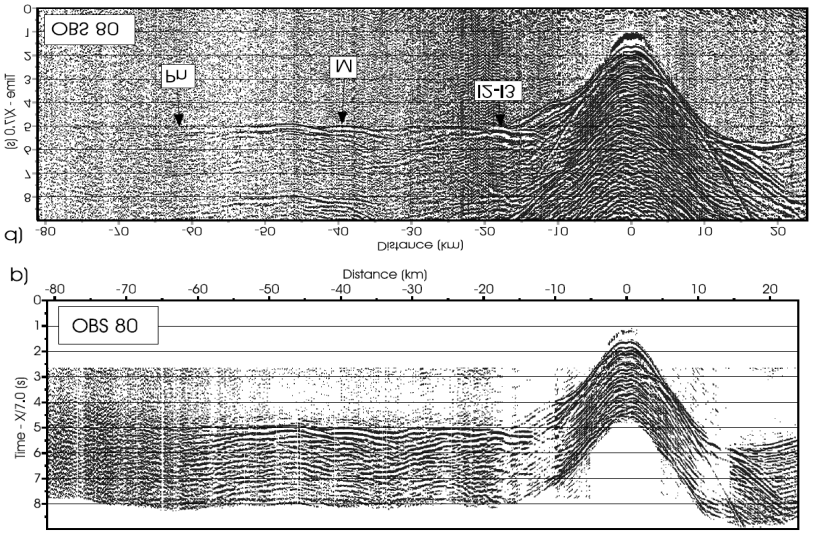

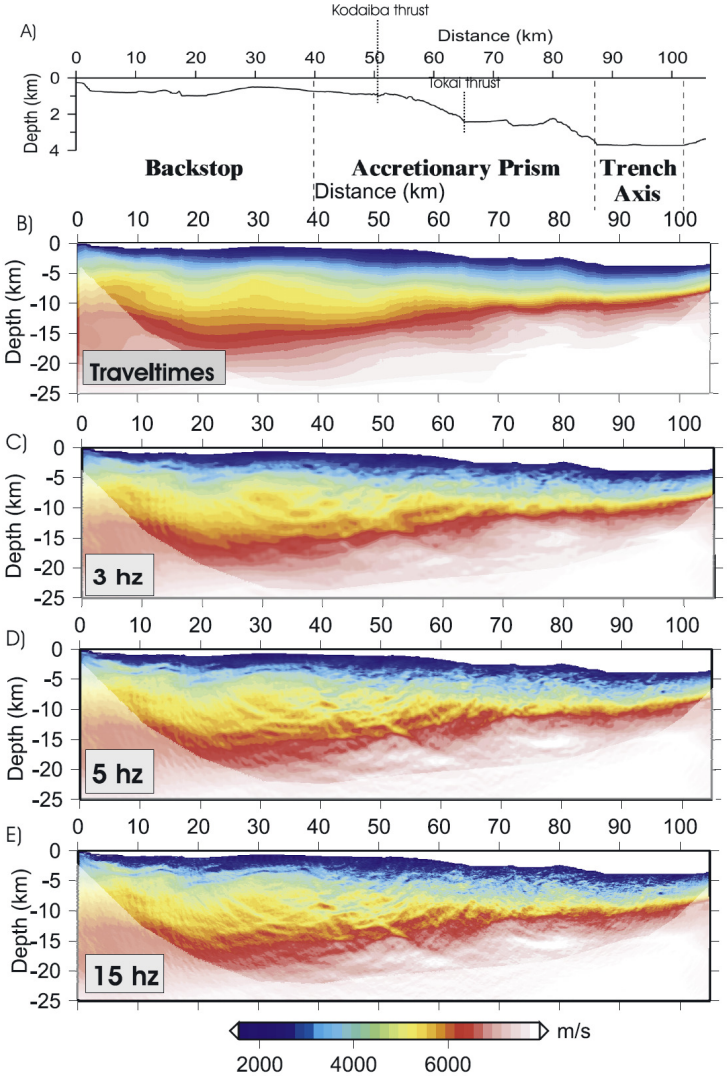

3D FWI : OBC Valhall application

- Valhall field : off-shore shallow-water in the North Sea. Over-pressured, under-saturated, Upper Cretaceous chalk reservoir (exploited since 1982)
- Shale at shallow depth : strong inprint of anisotropy in the seismic data
- 3D seismic : $\approx$ 50000 shots, 2414 permanent 4C sensors on the sea bed (OBC)

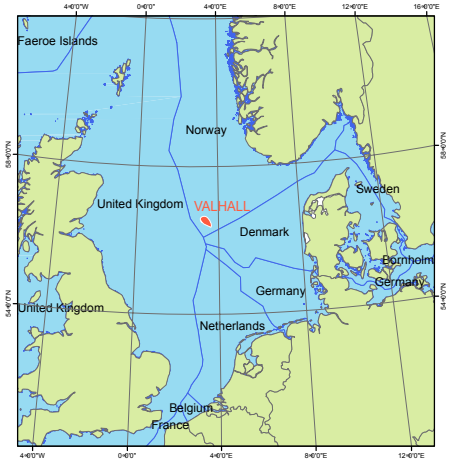

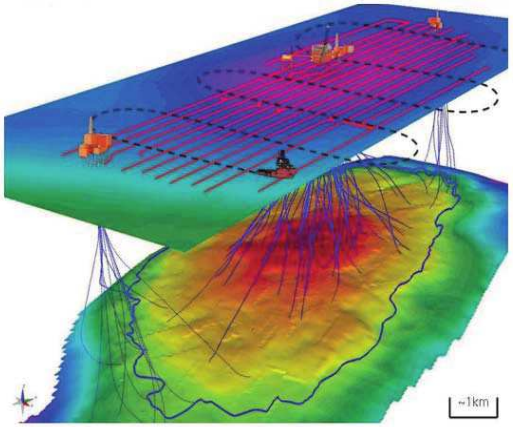

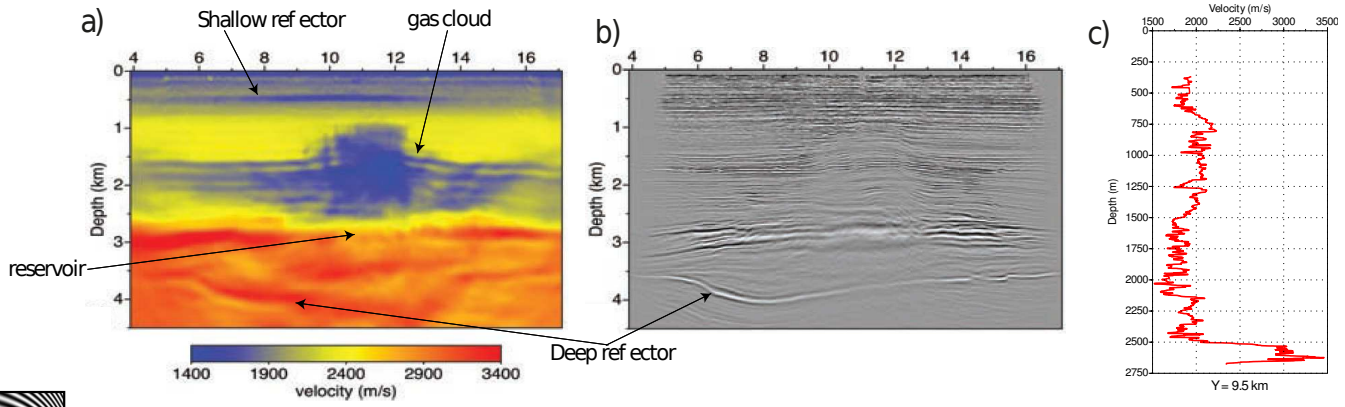

3D Acoustic isotropic FWI by Sirgue et al. (2010)

3D FWI : OBC Valhall application

Etienne et al. (2012); Hu et al. (2012)

Starting model from reflection tomography

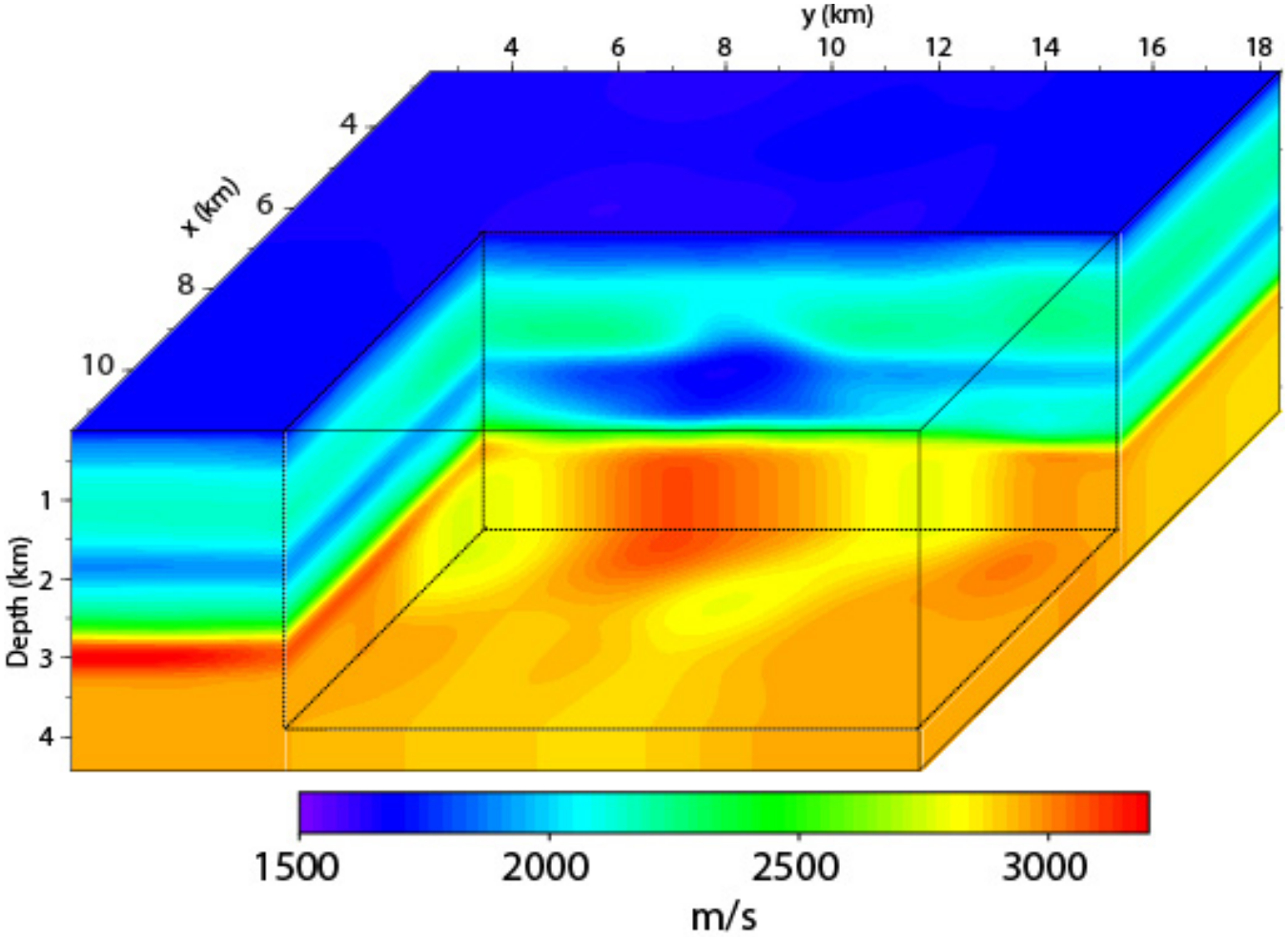

3D FWI : OBC Valhall application

Etienne et al. (2012); Hu et al. (2012)

FWI : [3.5,4] Hz

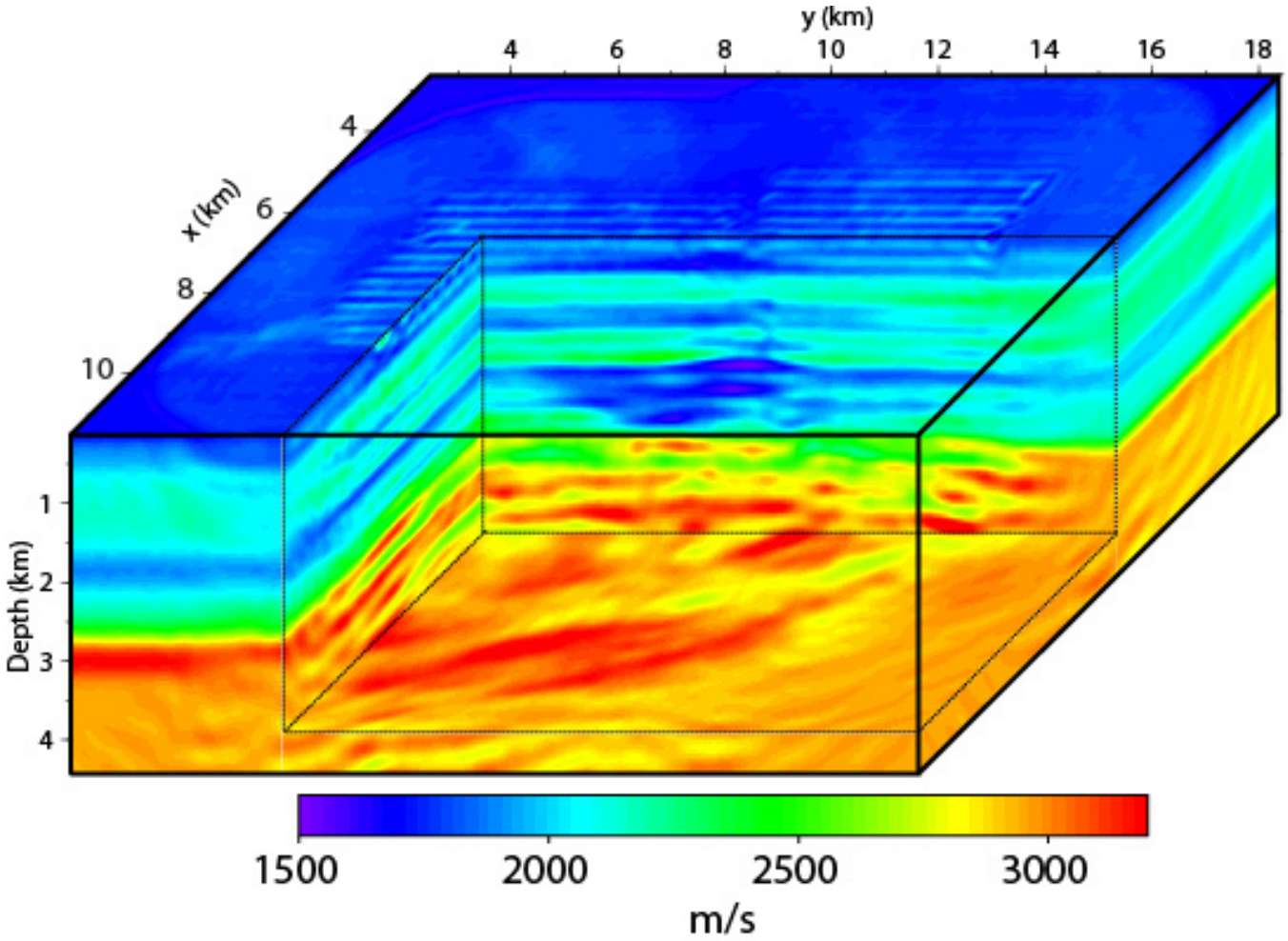

3D FWI : OBC Valhall application

Etienne et al. (2012); Hu et al. (2012)

FWI : [4,5] Hz

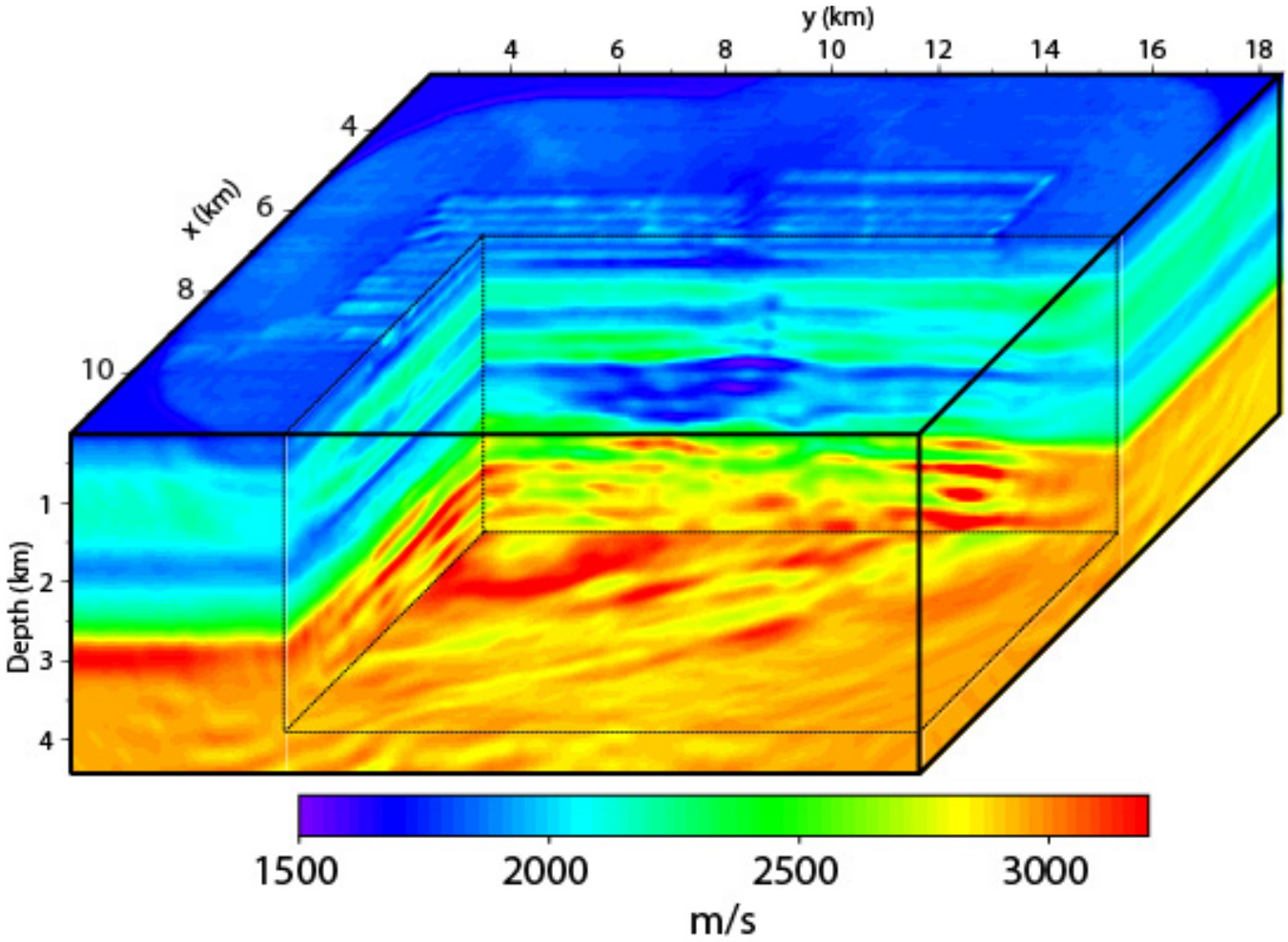

3D FWI : OBC Valhall application

Etienne et al. (2012); Hu et al. (2012)

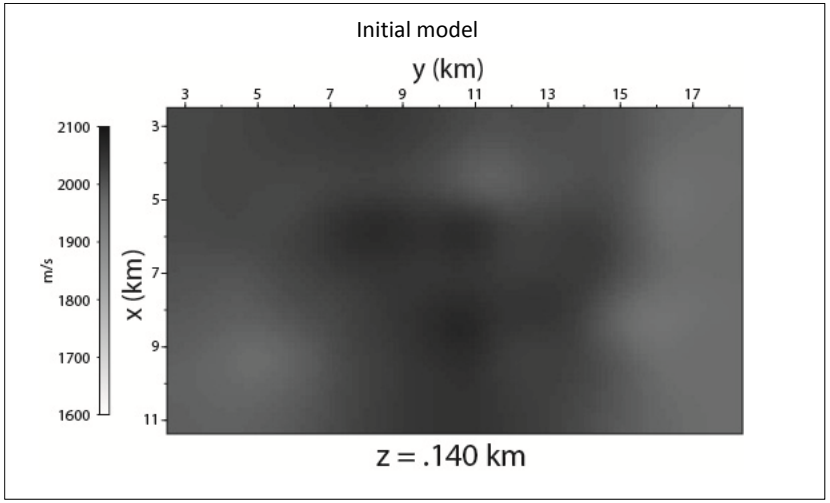

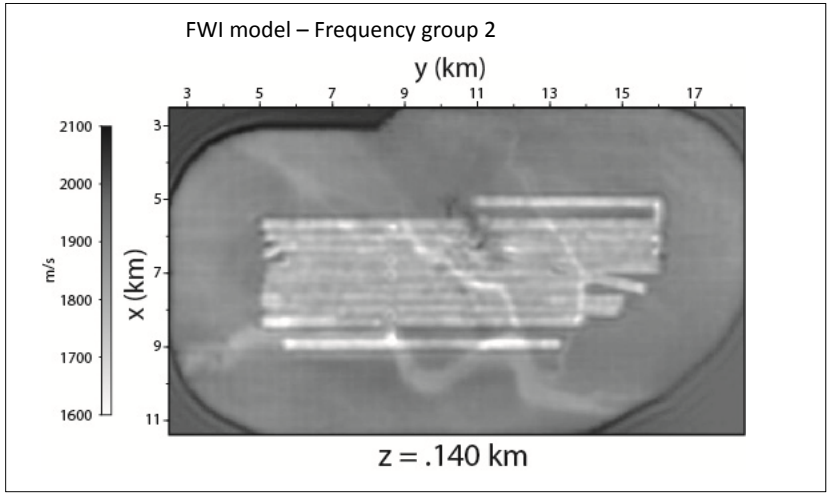

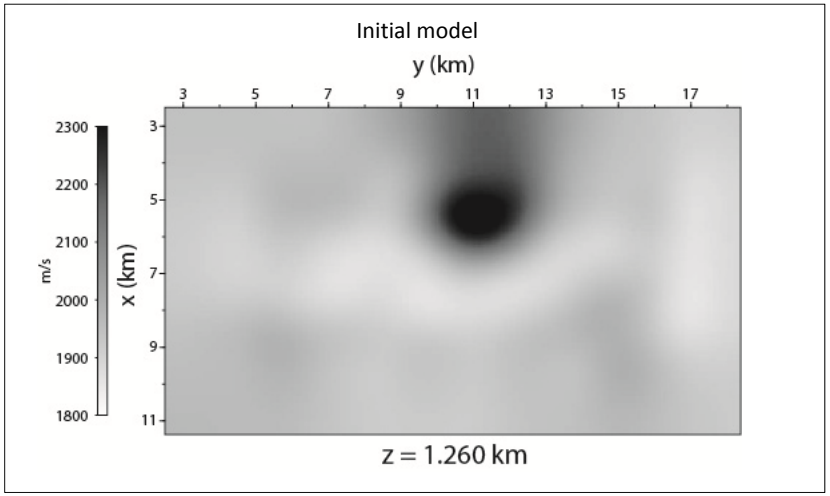

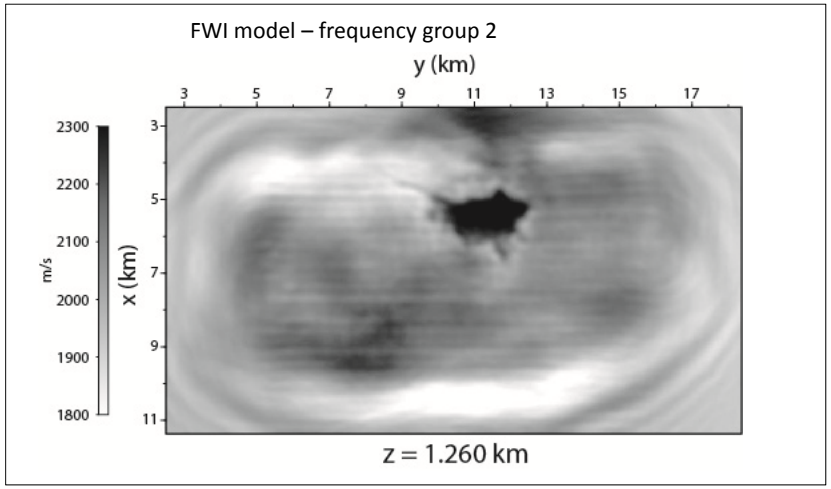

Remarks

- Most of the past and current applications rely on transitted energy
  - Cross-well data in pure transmission
  - Surface data taking benefit of direct, diving and refracted waves
- at depth, a migration-like behavior is observed : only high-wavenumber update

$\rightarrow$ how to take benefit from information coming from reflection energy

Outline

Velocity model building by reflected waves-based FWI

- Reemerging technique (Xu et al., 2012; Brossier et al., 2014) coming from Migration-Based Traveltime Tomography (Chavent et al., 1994)
- Initial assumption : scale separation between $m_0, \delta m$ and alternate update
  - Low-wavenumber background velocity model m_0 : RFWI
  - High-wavenumber perturbation model δm : migration or impedance FWI

Velocity model building by reflected waves-based FWI

- Reemerging technique (Xu et al., 2012; Brossier et al., 2014) coming from Migration-Based Traveltime Tomography (Chavent et al., 1994)
- Initial assumption : scale separation between $m_0, \delta m$ and alternate update
  - Low-wavenumber background velocity model m_0 : RFWI
  - High-wavenumber perturbation model δm : migration or impedance FWI
- Reflected-wave only misfit function (required to mute direct/diving waves)

$$C_{RFWI} = \frac{1}{2} \| d_{obs}^{refl} - d_{pred}^{refl}(m_0, \delta m) \|^2 \tag{6}$$

Velocity model building by reflected waves-based FWI

- Reemerging technique (Xu et al., 2012; Brossier et al., 2014) coming from Migration-Based Traveltime Tomography (Chavent et al., 1994)
- Initial assumption : scale separation between $m_0, \delta m$ and alternate update
  - Low-wavenumber background velocity model m_0 : RFWI
  - High-wavenumber perturbation model δm : migration or impedance FWI
- Reflected-wave only misfit function (required to mute direct/diving waves)

$$C_{RFWI} = \frac{1}{2}\|d_{obs}^{refl} - d_{pred}^{refl}(m_0, \delta m)\|^2 \tag{6}$$

Gradient for m_0:

$$G_{RFWI} = u_0 \star \delta\lambda + \delta u \star \lambda_0 \tag{7}$$

where

$$\begin{cases} u_0\text{: background part of incident field,} \\ \delta\lambda\text{: scattered part of adjoint field,} \\ \delta u\text{: scattered part of incident field,} \\ \lambda_0\text{: background part of adjoint field} \end{cases}$$

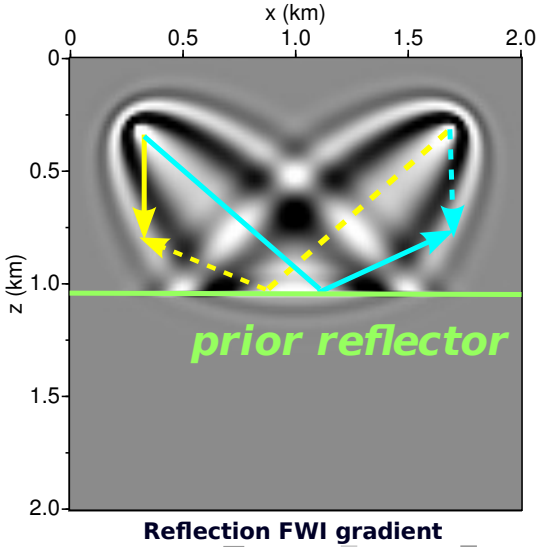

Reflection FWI gradient

Velocity model building by reflected waves-based FWI

$$C_{RFWI} = \frac{1}{2}\|d_{obs}^{refl} - d_{pred}^{refl}(m_0, \delta m)\|^2 \qquad G_{RFWI} = u_0 \star \delta\lambda + \delta u \star \lambda_0$$

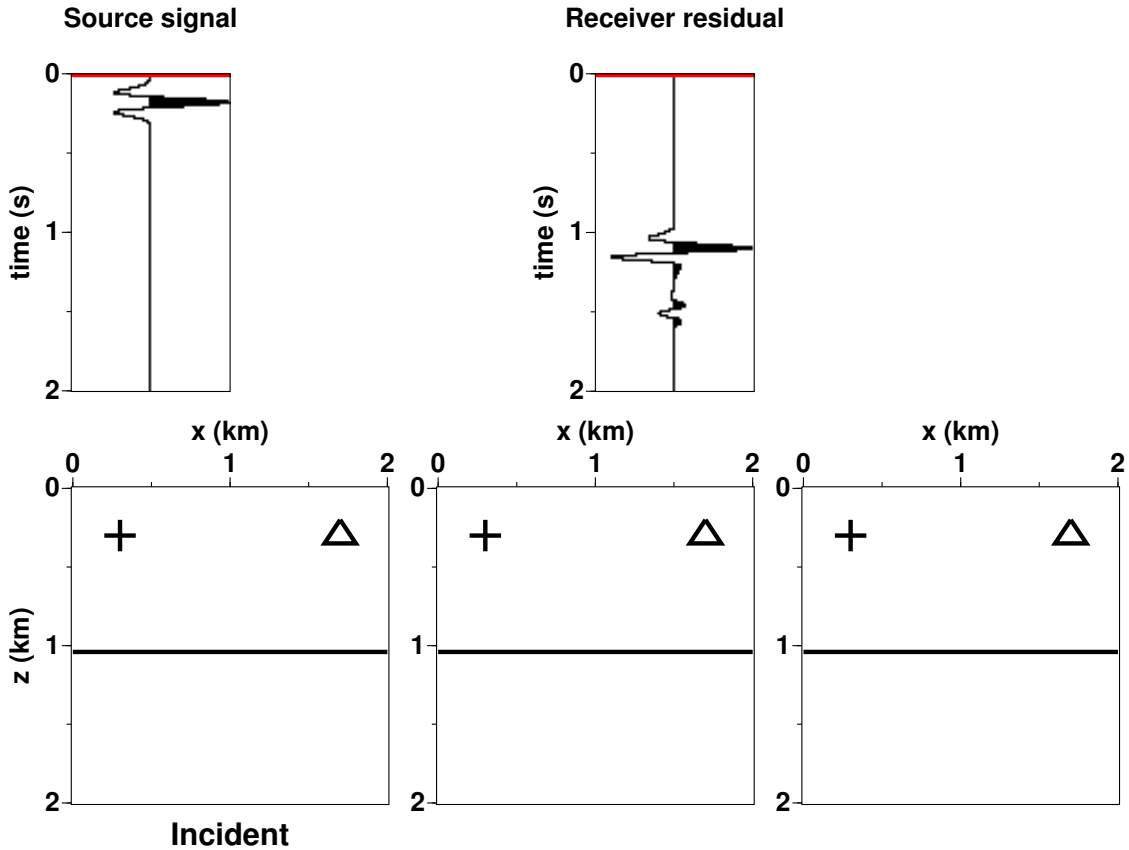

Time = .008 s

Velocity model building by reflected waves-based FWI

$$C_{RFWI} = \frac{1}{2}\|d_{obs}^{refl} - d_{pred}^{refl}(m_0, \delta m)\|^2 \qquad G_{RFWI} = u_0 \star \delta\lambda + \delta u \star \lambda_0$$

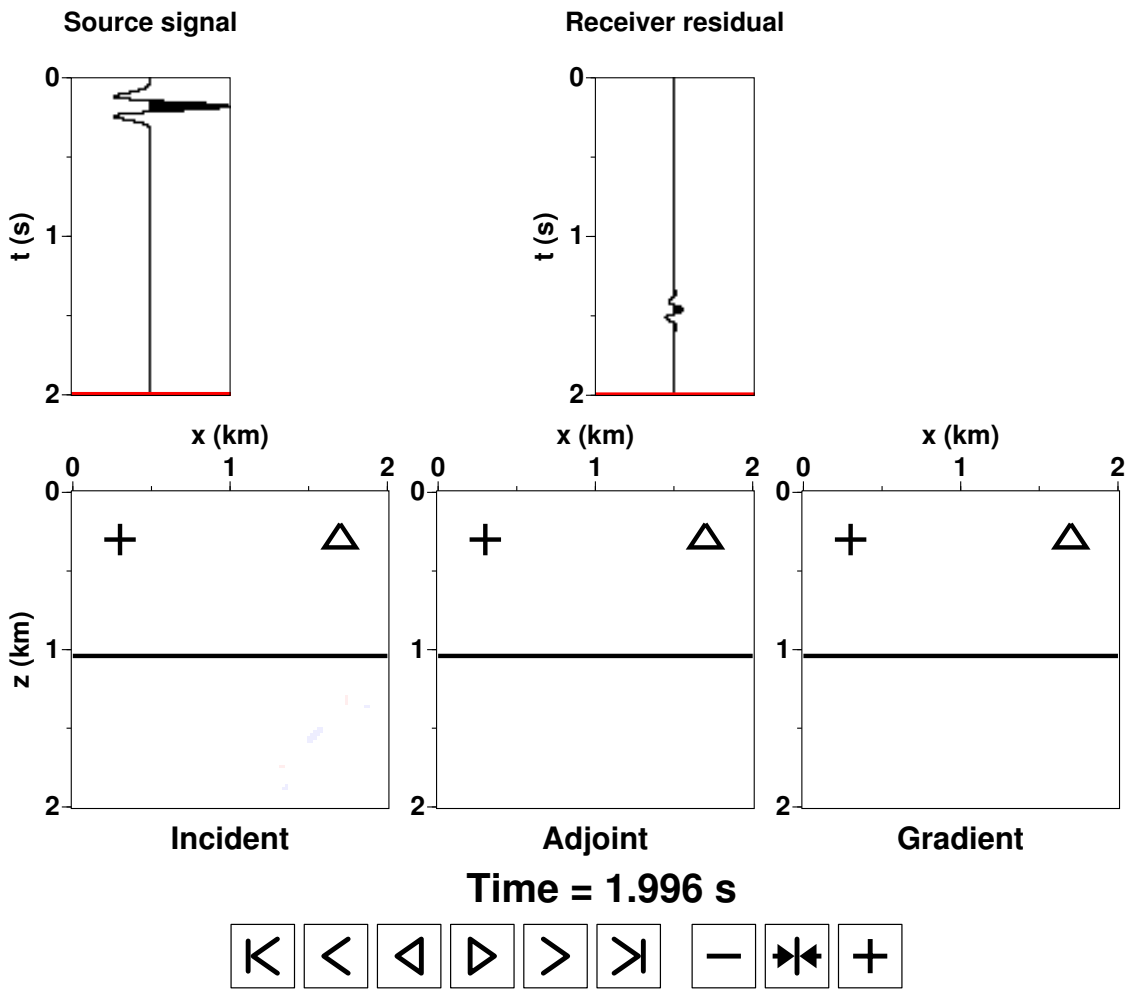

Velocity model building by reflected waves-based FWI

- RFWI focuses on reflected waves only, discarding the low-wavenumber information carried out by transmitted waves.
- Nowadays, very long-offset and wide azimuth acquisitions are well designed, providing the possibility to image the subsurface by including diving waves and postcritical reflections.

$\rightarrow$ need to combine diving waves and reflected waves

Outline

Sum of the Two ?

- Inverting all types of waves, still considering explicitely the reflectivity.

$$C_{FWIwithReflectivity} = \frac{1}{2}\|d_{obs}^{div} - d_{pred}^{div}(m_0) \; + \; d_{obs}^{refl} - d_{pred}^{refl}(m_0, \delta m)\|^2 \tag{8}$$

Sum of the Two ?

- Inverting all types of waves, still considering explicitely the reflectivity.

$$C_{FWIwithReflectivity} = \frac{1}{2}\|d_{obs}^{div} - d_{pred}^{div}(m_0) \; + \; d_{obs}^{refl} - d_{pred}^{refl}(m_0, \delta m)\|^2 \tag{8}$$

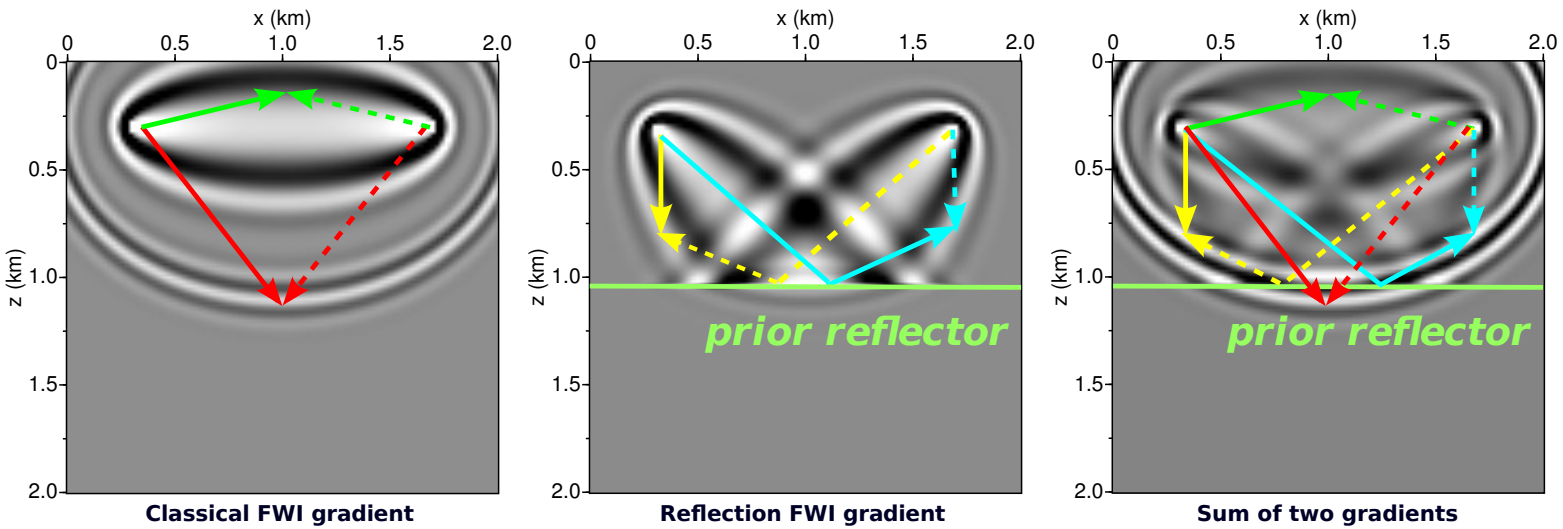

- Problem : The 1st-order isochrones generated by reflected waves are also injected into the gradient, which damage our low-wavenumber macromodel building.

Sum of the Two ?

- Inverting all types of waves, still considering explicitely the reflectivity.

$$C_{FWIwithReflectivity} = \frac{1}{2}\|d_{obs}^{div} - d_{pred}^{div}(m_0) \; + \; d_{obs}^{refl} - d_{pred}^{refl}(m_0, \delta m)\|^2 \tag{8}$$

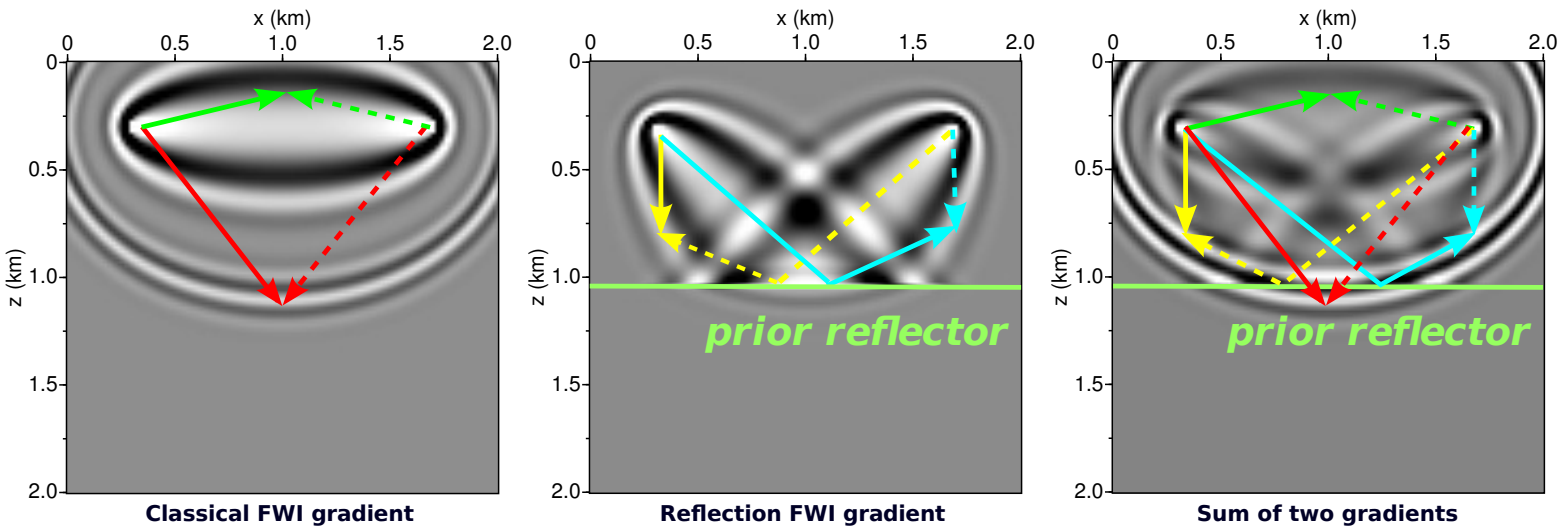

Classical FWI gradient | Reflection FWI gradient | Sum of two gradients

- Problem : The 1st-order isochrones generated by reflected waves are also injected into the gradient, which damage our low-wavenumber macromodel building.
  $\rightarrow$ need for a smarter combination !

Outline

Formalism of the Joint FWI

Zhou et al. (2014)

- Misfit function (explicit split between transmitted and reflected energy):

$$C_{JointFWI} = \frac{1}{2}\| W^d \left(d^{div}_{obs} - d^{div}_{pred}(m_0) \right) \|^2 + \frac{1}{2}\| W^r \left(d^{refl}_{obs} - d^{refl}_{pred}(m_0, \delta m) \right) \|^2 \quad (9)$$

where W^d, W^r are weighting operators for diving and reflected waves, respectively.

- Gradient:

$$G_{JointFWI} = u_0 \star \lambda^d_0 + u_0 \star \delta\lambda^r + \delta u \star \lambda^r_0 + \delta u \star \delta\lambda^r \quad (10)$$

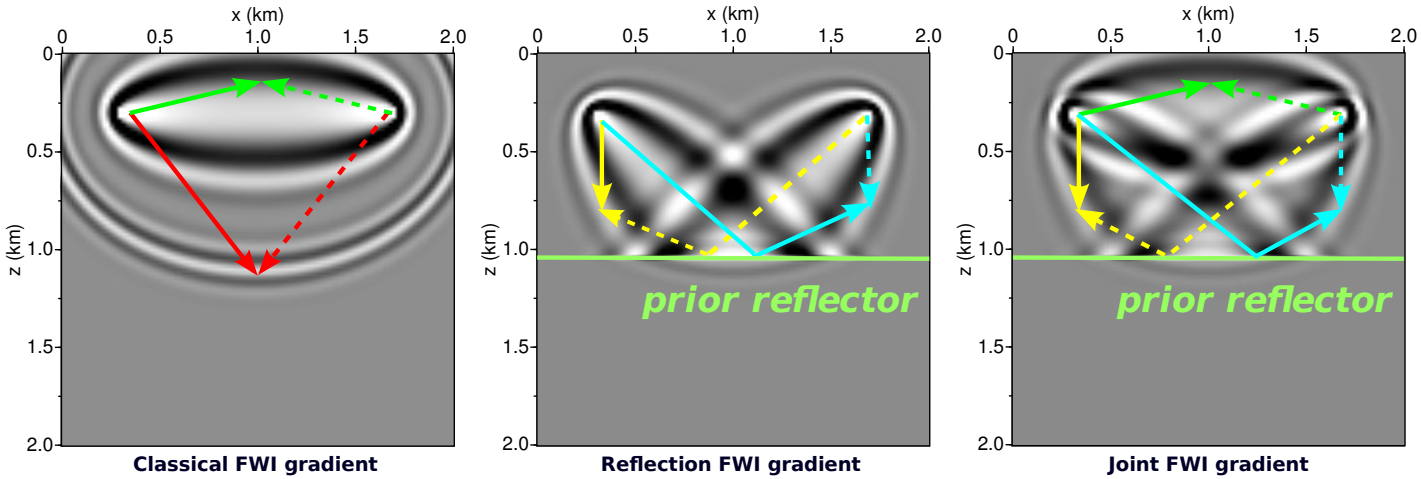

→ low-wavenumber components only thanks to explicit separation

What happens in a 2 reflectors case ?

$$G_{JointFWI} = u_0 \star \lambda_0^d + u_0 \star \delta\lambda^r + \delta u \star \lambda_0^r + \delta u \star \delta\lambda^r \quad (11)$$

- the presence of δm generates multi-scattered waves, leading to unphysical higher-order isochrones
  $\rightarrow$ same effects that classical migration edge-artifacts
- stacking over sources and receivers should mitigate their energy
- appropriate parametrization is important

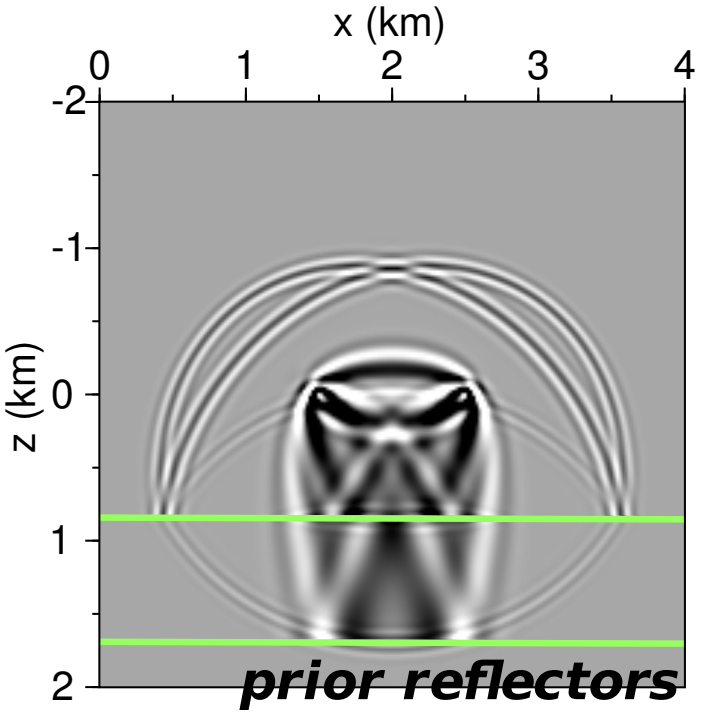

Outline

Importance of parametrization

$V_P - \rho$ parameterization:

- (Left) V_P: Isotropic pattern for V_P diffractor. Scattered wave is equally energetic from short to wide θ.
- (Right) ρ: Scattering at short-to-intermediate θ.
- Cross-talks of V_P and ρ at short-to-intermediate θ.

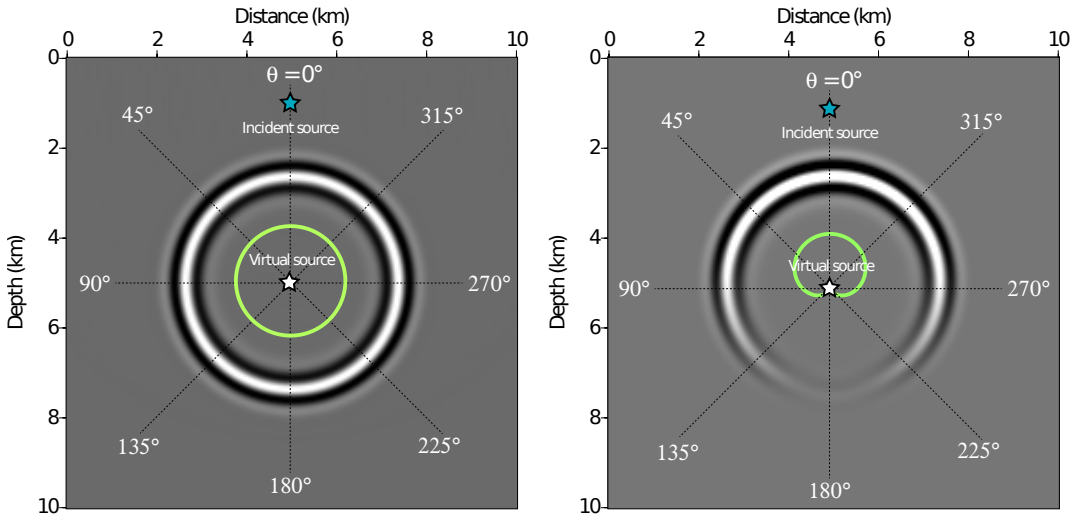

Vp-ρ, Vp inclusion **Vp-ρ, ρ inclusion**

Importance of parametrization

$V_P - \rho$ parameterization:

- (Left) V_P: Isotropic pattern for V_P diffractor. Scattered wave is equally energetic from short to wide θ.
- (Right) ρ: Scattering at short-to-intermediate θ.
- Cross-talks of V_P and ρ at short-to-intermediate θ.

$V_P - I_P$ parameterization:

- (Left) V_P: Scattering at intermediate-to-wide θ.
- (Right) I_P: Scattering at short-to-intermediate θ.
- Less cross-talks and keeping low wavenumbers in V_P.

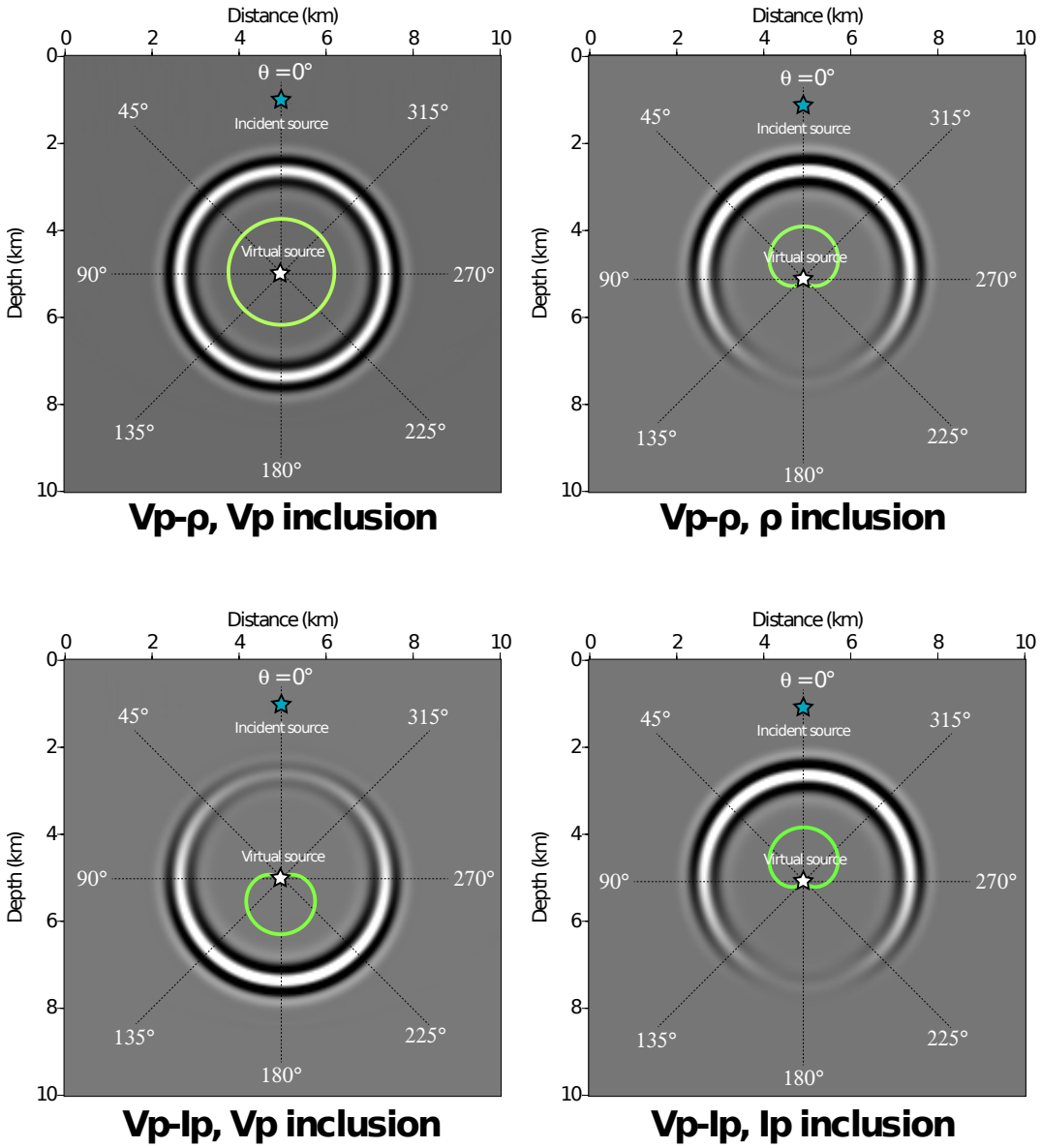

from Operto et al. (2013)

Importance of parametrization

$V_P - \rho$ parameterization:

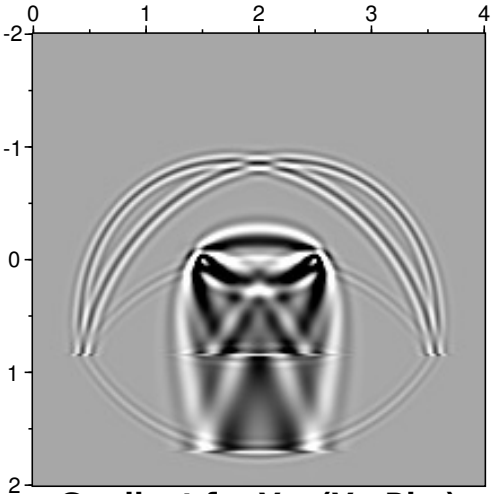

Gradient for Vp (Vp-Rho)

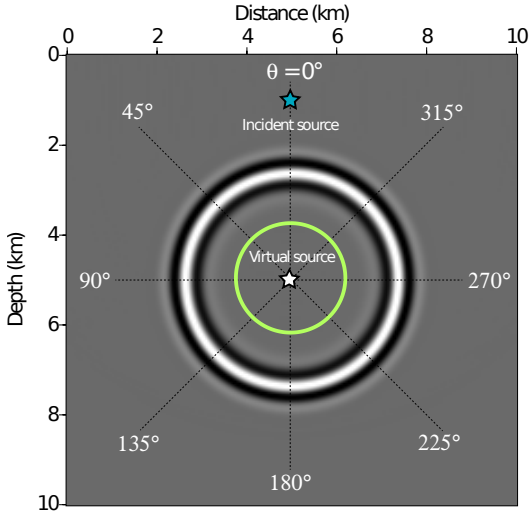

Vp-ρ, Vp inclusion

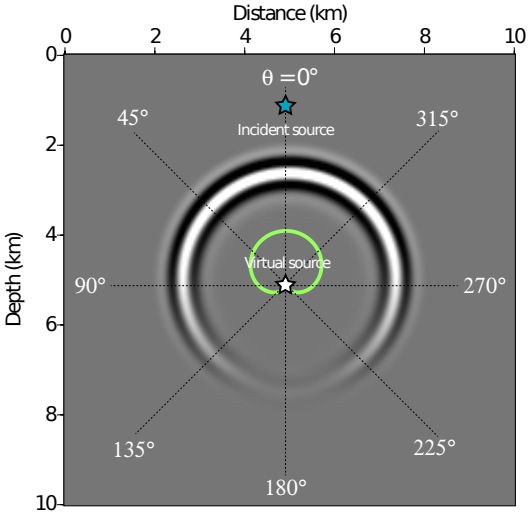

Vp-ρ, ρ inclusion

$V_P - I_P$ parameterization:

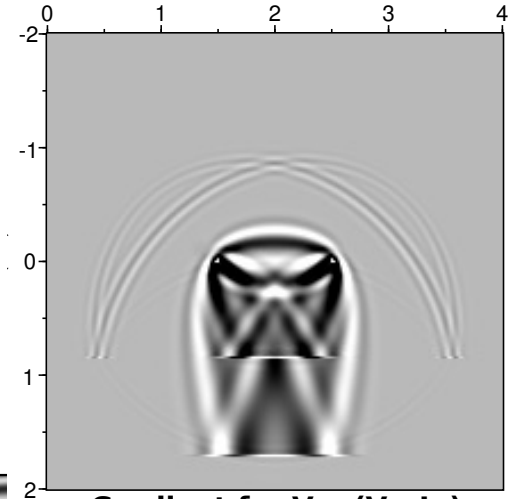

Gradient for Vp (Vp-Ip)

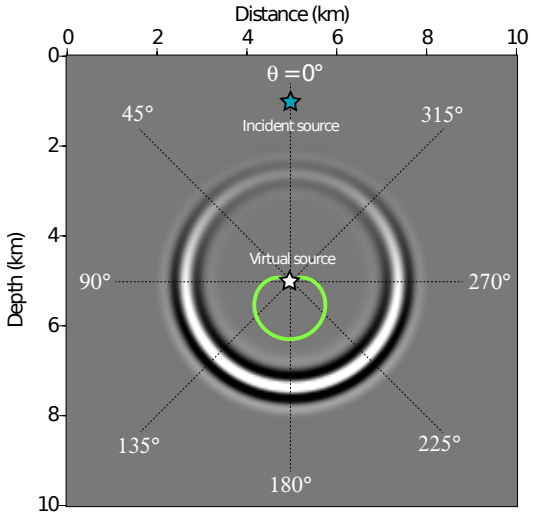

Vp-Ip, Vp inclusion

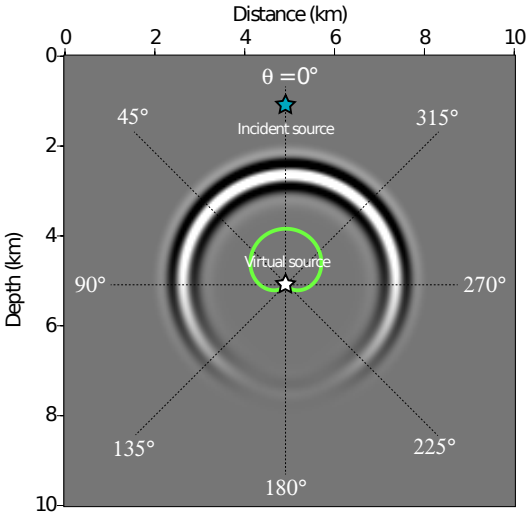

Vp-Ip, Ip inclusion

from Operto et al. (2013)

Perturbation imaging by impedance Inversion

- The high-wavenumber perturbation δm is built through I_P inversion in FWI.
- Misfit function:

$$C_{I_P} = \frac{1}{2} \| W^r \left(d_{obs}^{refl} - d_{pred}^{refl}(m_0, \delta m) \right) \|^2 \tag{12}$$

- Gradient:

$$G_{I_P} = u_0 \star \lambda_0^r \tag{13}$$

Starting from a smooth I_P model

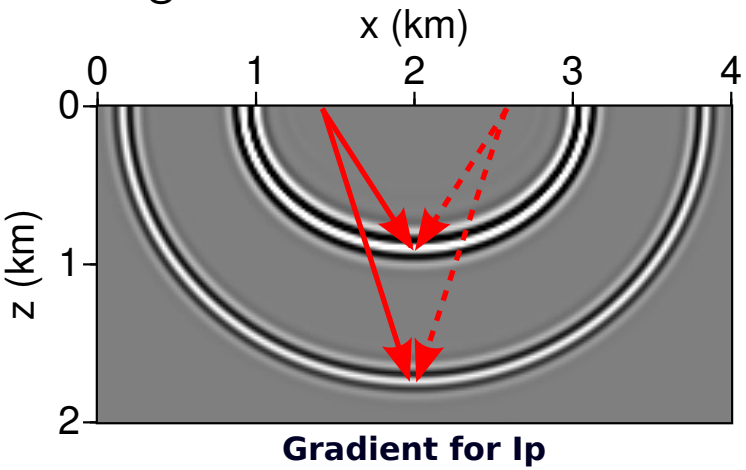

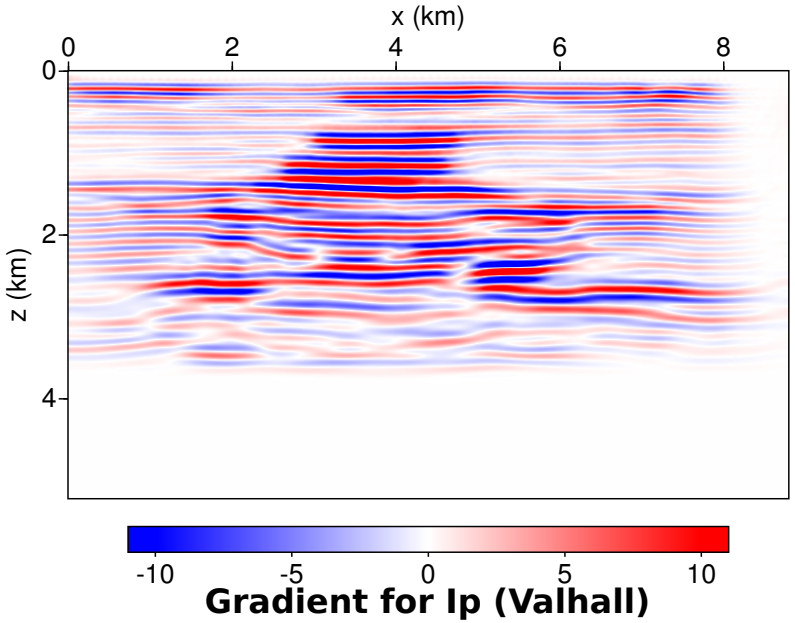

Outline

Algorithm for the whole Workflow

Smooth V_P and I_P initials

repeat

USE initial (or updated) Vp
USE initial Ip, NO reflectivity
DO Ip inversion
GET reflectivity in Ip
(high-wavenumber content)

USE initial (or updated) Vp
USE Ip with reflectivity
DO Vp inversion
GET updated Vp
(low-wavenumber content)

until convergence

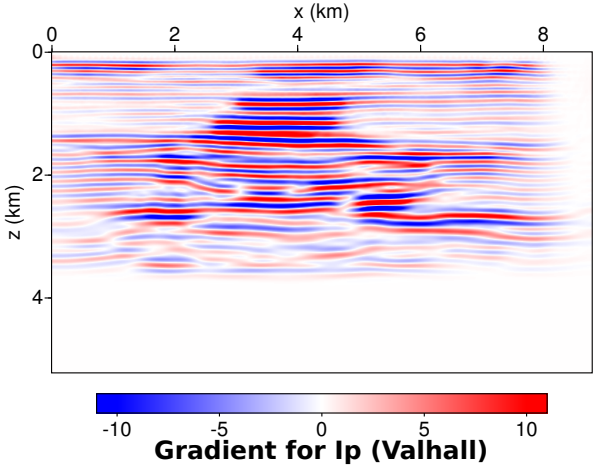

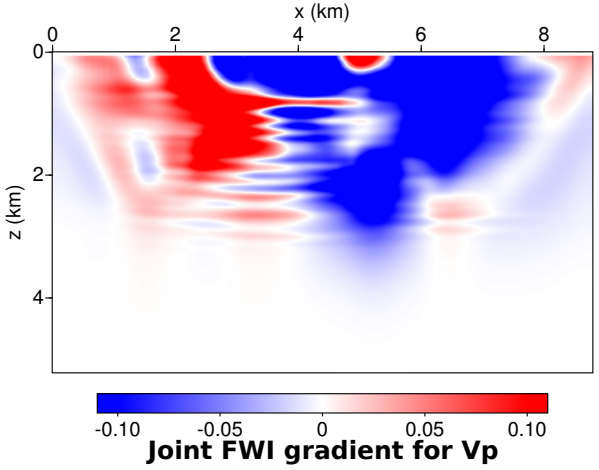

Outline

Models and Configurations

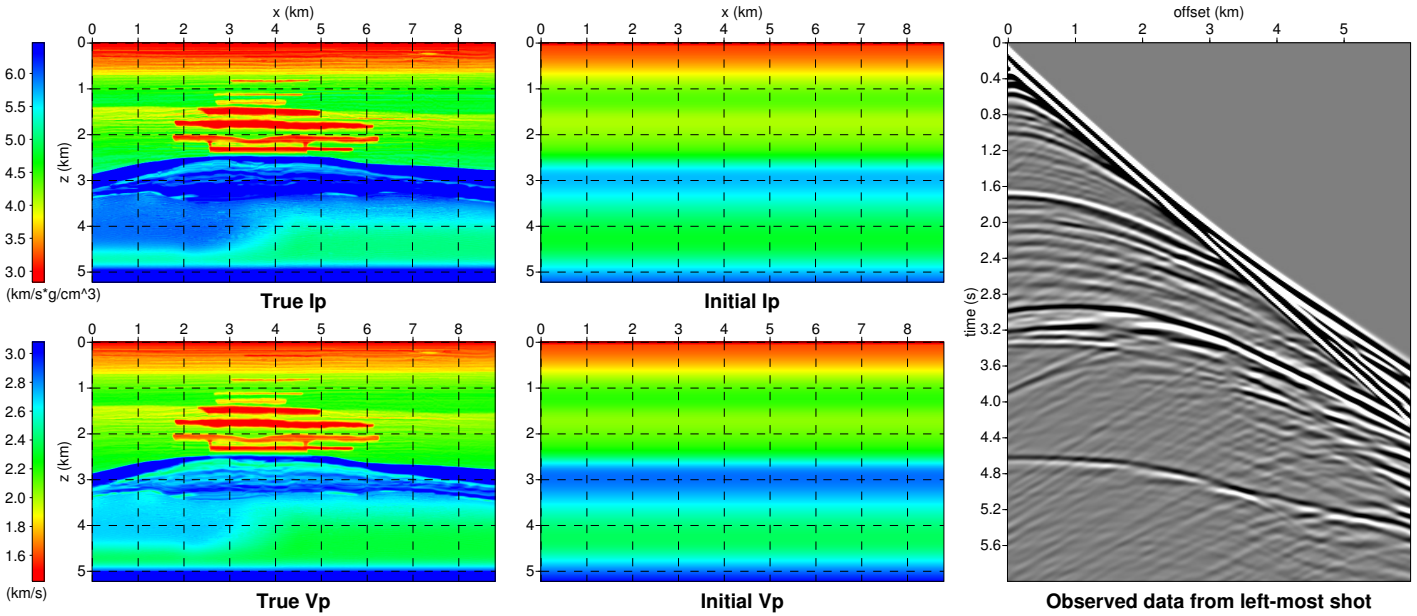

Max. offset: 6km

Frequency band: 2Hz $\sim$ 12.5Hz

Peak freq: 6.25Hz

Results during the iterative process

Alternate update of reflectivity (through impedance) and velocity

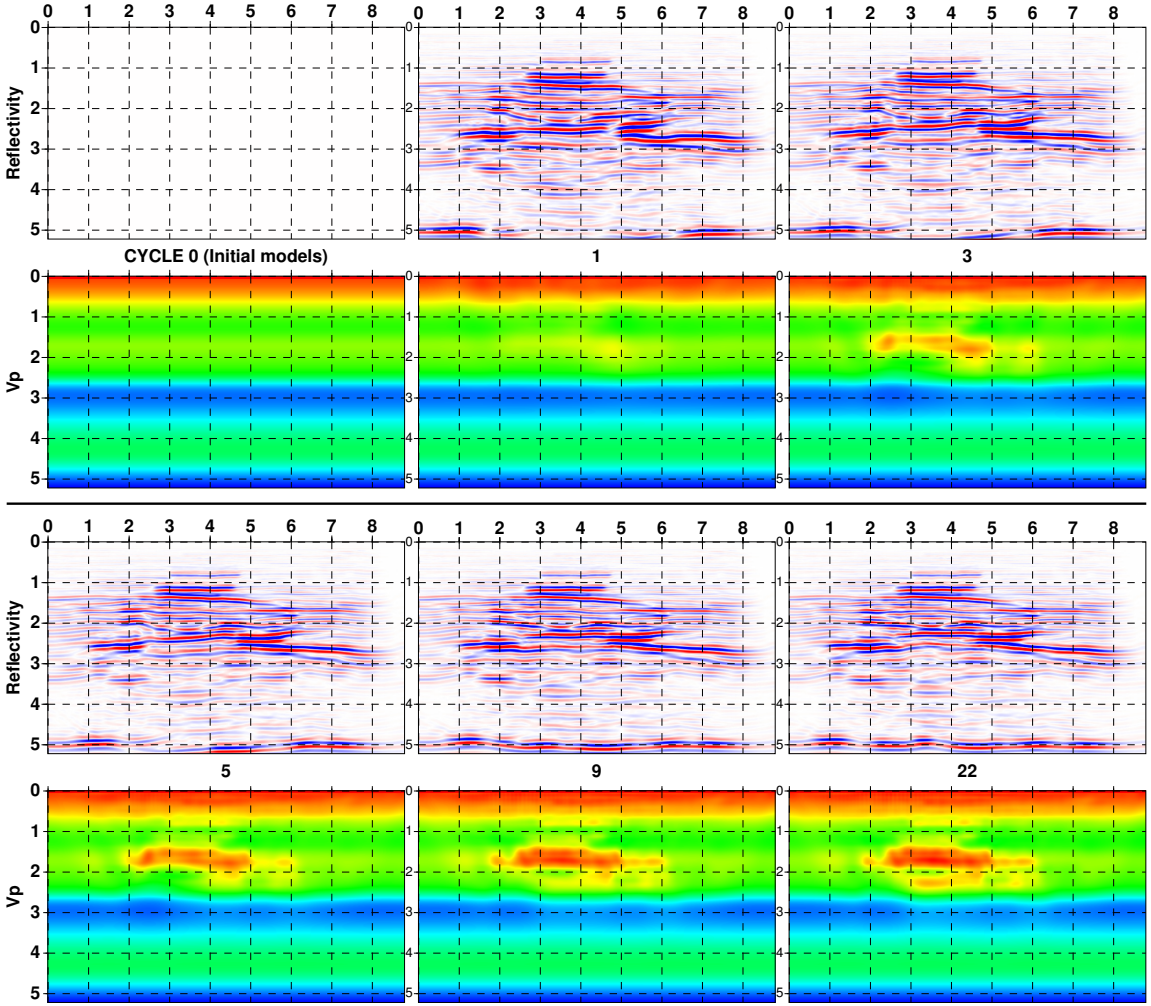

Final results and comparison

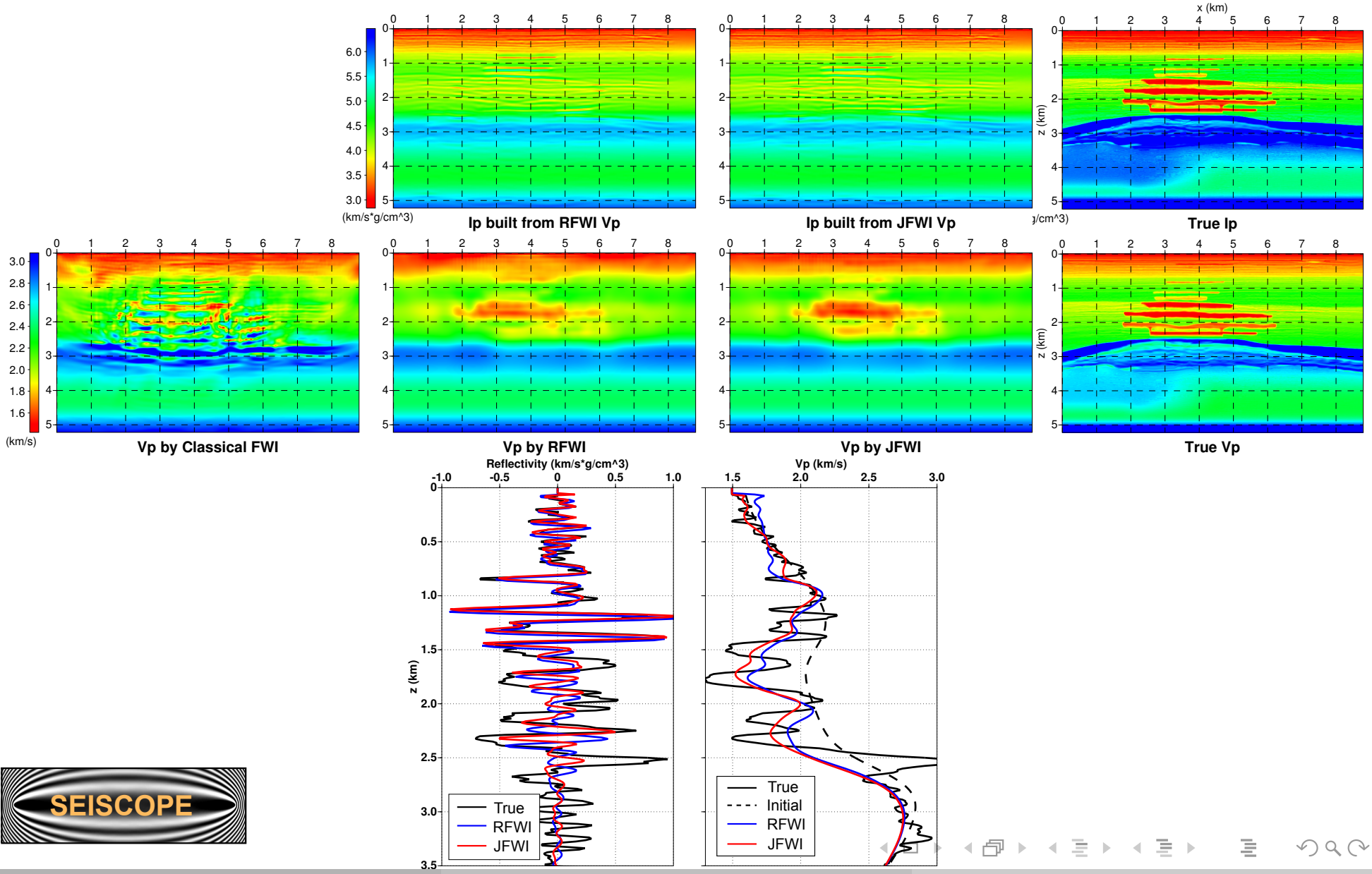

Final Impedance estimation : benefit of JFWI

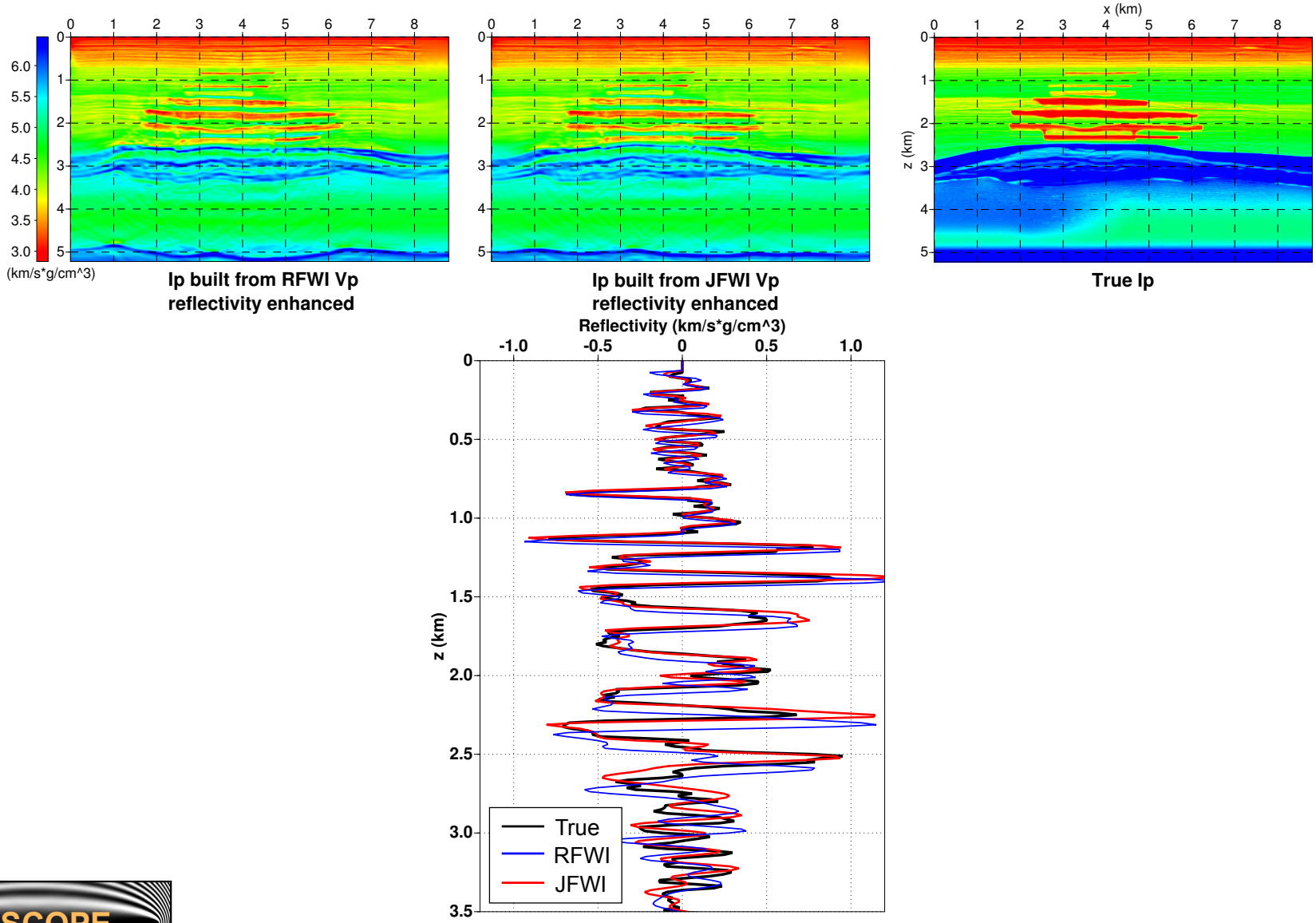

Data fit

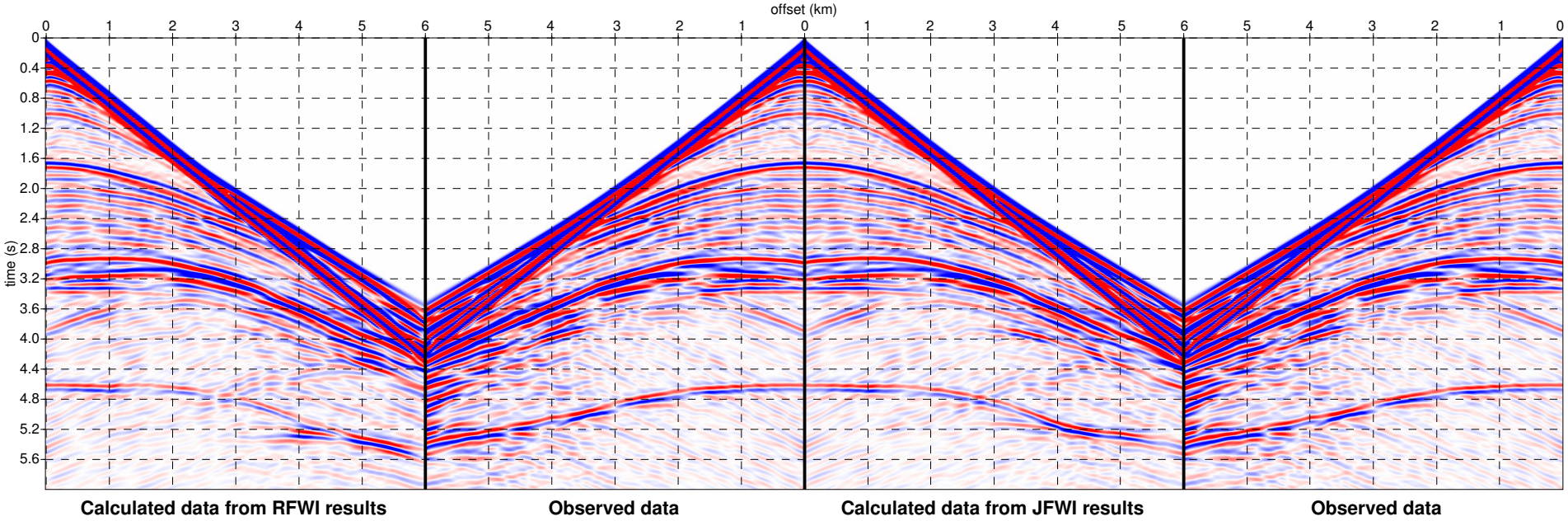
offset (km)
time (s)
Calculated data from RFWI results
Observed data
Calculated data from JFWI results
Observed data

Outline

Conclusion

- Despite a number of success to real data, classical FWI formulation is unable to use reflected waves to update the full wavenumber spectrum : problem at depth when lack of diving-wave coverage.
- Using an explicit wavenumber separation of the model representation and alternate updates
  - Reflected-wave FWI allows to take benefit of reflected wave information for velocity model buidling, but discard a large part of recorded energy
  - Our joint FWI scheme allows to fully benefit from both the diving waves and reflected waves information
- RFWI and JFWI rely on an explicit scale separation. V_P–I_P parametrization is the most suitable choice to honor this scale separation.
- Applications on the synthetic Valhall shows the benefit of the JFWI scheme over RFWI.

Thank you for your attention

- National computing centers from GENCI: IDRIS and CINES (projects GAO2280 and CUF1954).
- Local computing center CIMENT (OSUG)
- SEICOPE sponsors : `http://seiscope2.osug.fr`

Brossier, R., Operto, S., and Virieux, J. (2014). Velocity model building from seismic reflection data by full waveform inversion. *Geophysical Prospecting*, doi = 10.1049/ip-f-1.1983.0003,.

Chavent, G., Clément, F., and Gòmez, S. (1994). Automatic determination of velocities via migration-based traveltime waveform inversion: A synthetic data example. *SEG Technical Program Expanded Abstracts 1994*, pages 1179–1182.

Devaney, A. J. (1982). A filtered backprojection algorithm for diffraction tomography. *Ultrasonic Imaging*, 4:336–350.

Etienne, V., Hu, G., Operto, S., Virieux, J., Barkved, O., and Kommedal, J. (2012). Three-dimensional acoustic full waveform inversion: algorithm and application to Valhall. In *Expanded Abstracts, 74th Annual EAGE Conference & Exhibition, Copenhagen*. EAGE.

Hu, G., Etienne, V., Castellanos, C., Operto, S., Brossier, R., and Virieux, J. (2012). Assessment of 3D acoustic isotropic full waveform inversion of wide-azimuth OBC data from Valhall. In *SEG Technical Program Expanded Abstracts 2012*, pages 1–6.

Lailly, P. (1983). The seismic inverse problem as a sequence of before stack migrations. In Bednar, R. and Weglein, editors, *Conference on Inverse Scattering, Theory and application, Society for Industrial and Applied Mathematics, Philadelphia*, pages 206–220.

Operto, S., Virieux, J., Dessa, J. X., and Pascal, G. (2006). Crustal imaging from multifold ocean bottom seismometers data by frequency-domain full-waveform tomography: application to the eastern Nankai trough. *Journal of Geophysical Research*, 111(B09306):doi:10.1029/2005JB003835.

Pratt, R. G. and Worthington, M. H. (1990). Inverse theory applied to multi-source cross-hole tomography. Part I: acoustic wave-equation method. *Geophysical Prospecting*, 38:287–310.

Tarantola, A. (1984). Inversion of seismic reflection data in the acoustic approximation. *Geophysics*, 49(8):1259–1266.

Virieux, J. and Operto, S. (2009). An overview of full waveform inversion in exploration geophysics. *Geophysics*, 74(6):WCC1–WCC26.

Wu, R. S. and Toksöz, M. N. (1987). Diffraction tomography and multisource holography applied to seismic imaging. *Geophysics*, 52:11–25.

Xu, S., Wang, D., Chen, F., Lambaré, G., and Zhang, Y. (2012). Inversion on reflected seismic wave. *SEG Technical Program Expanded Abstracts 2012*, pages 1–7.

Zhou, W., Brossier, R., Operto, S., and Virieux, J. (2014). Combining diving and reflected waves for velocity model building by waveform inversion. In *Expanded Abstracts, 76th Annual EAGE Meeting (Amsterdam)*.